

5-06-2024

Giuseppe Di Somma



Istituto Nazionale di Fisica Nucleare



UNIVERSITÀ DI PISA



Comparative analysis of local angular rotation between the ring laser gyroscope GINGERINO and GNSS stations

Giuseppe Di Somma^{1,2,a} , Nicolò Beverini¹, Giorgio Carelli^{1,2}, Simone Castellano^{2,3}, Roberto Devoti⁴, Enrico Maccioni^{1,2}, Paolo Marsili^{1,2}, Angela D. V. Di Virgilio²

¹ Dipartimento di Fisica, Università di Pisa, largo B. Pontecorvo 3, 56127 Pisa, Italy

² Istituto Nazionale di Fisica Nucleare (INFN), sez. di Pisa, largo B. Pontecorvo 3, 56127 Pisa, Italy

³ Gran Sasso Science Institute, Viale Francesco Crispi 7, 67100 L'Aquila, AQ, Italy

⁴ Istituto Nazionale di Geofisica e Vulcanologia, Sez. ONT, Sede di Roma, Italy

Received: 30 August 2023 / Accepted: 31 January 2024

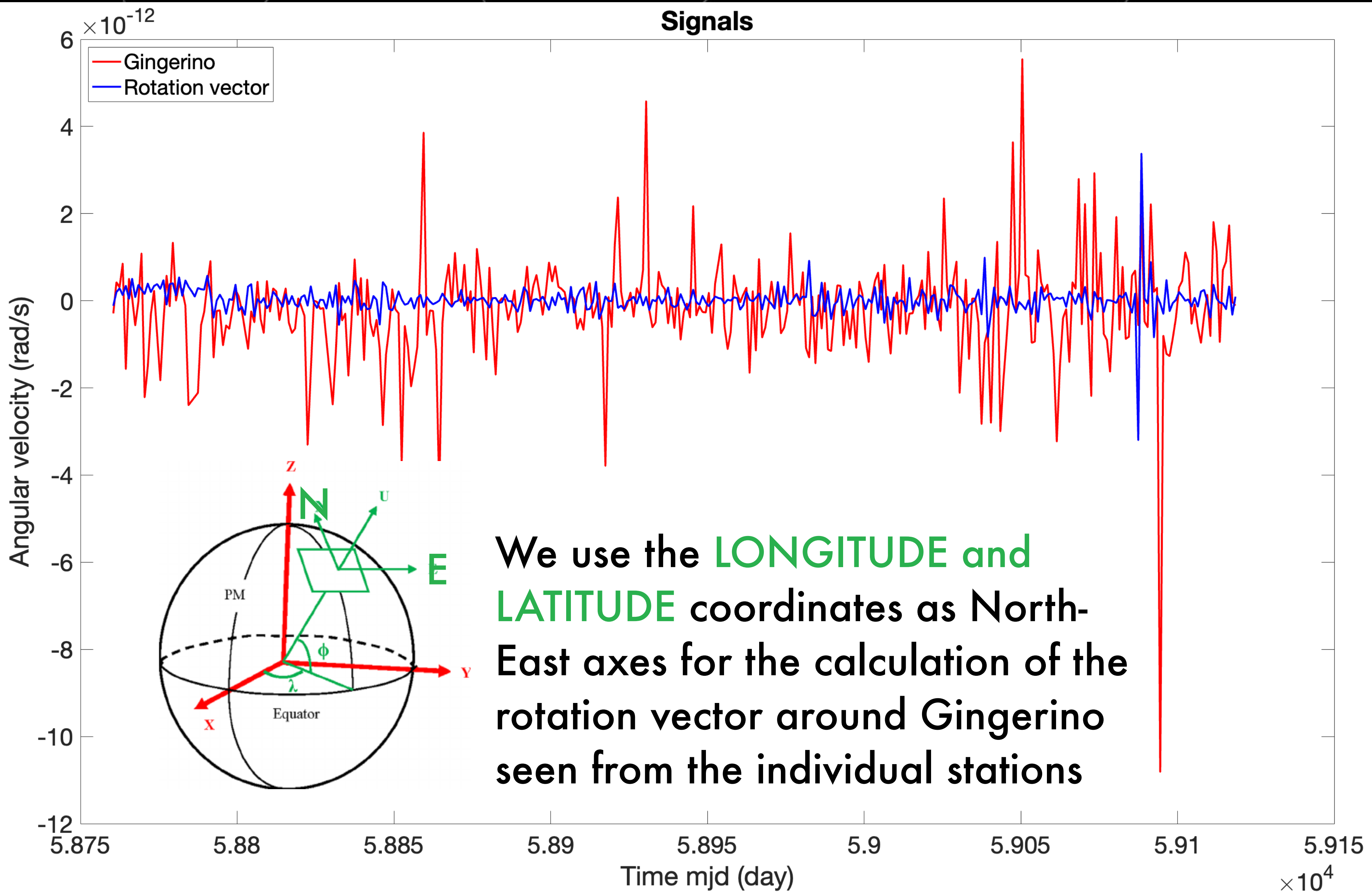
© The Author(s), under exclusive licence to Società Italiana di Fisica and Springer-Verlag GmbH Germany, part of Springer Nature 2024

Abstract The study of local deformations is a hot topic in geodesy. Local rotations of the crust around the vertical axis can be caused by deformations. In the Gran Sasso area, the ring laser gyroscope GINGERINO and the GNSS array are operative. One year of data of GINGERINO is compared with the ones from the GNSS stations, homogeneously selected around the position of GINGERINO, aiming at looking for rotational signals with period of days common to both systems. At that purpose the rotational component of the area circumscribed by the GNSS stations has been evaluated and compared with the GINGERINO data. The coherences between the signals show structures that even exceed 60% coherence over the 6–60 days period; this unprecedented analysis is validated by two different methods that evaluate the local rotation using the GNSS stations. The analysis reveals that the shared rotational signal's amplitude in both instruments is approximately 10^{-13} rad/s, an order of magnitude lower than the amplitudes of the signals examined. The comparison of the ring laser data with GNSS antennas provides evidence of the validity of the ring laser data for very low frequency investigation, essential for fundamental physics test.

The presentation is based on
an article we published
Please refer to this link for
more details:

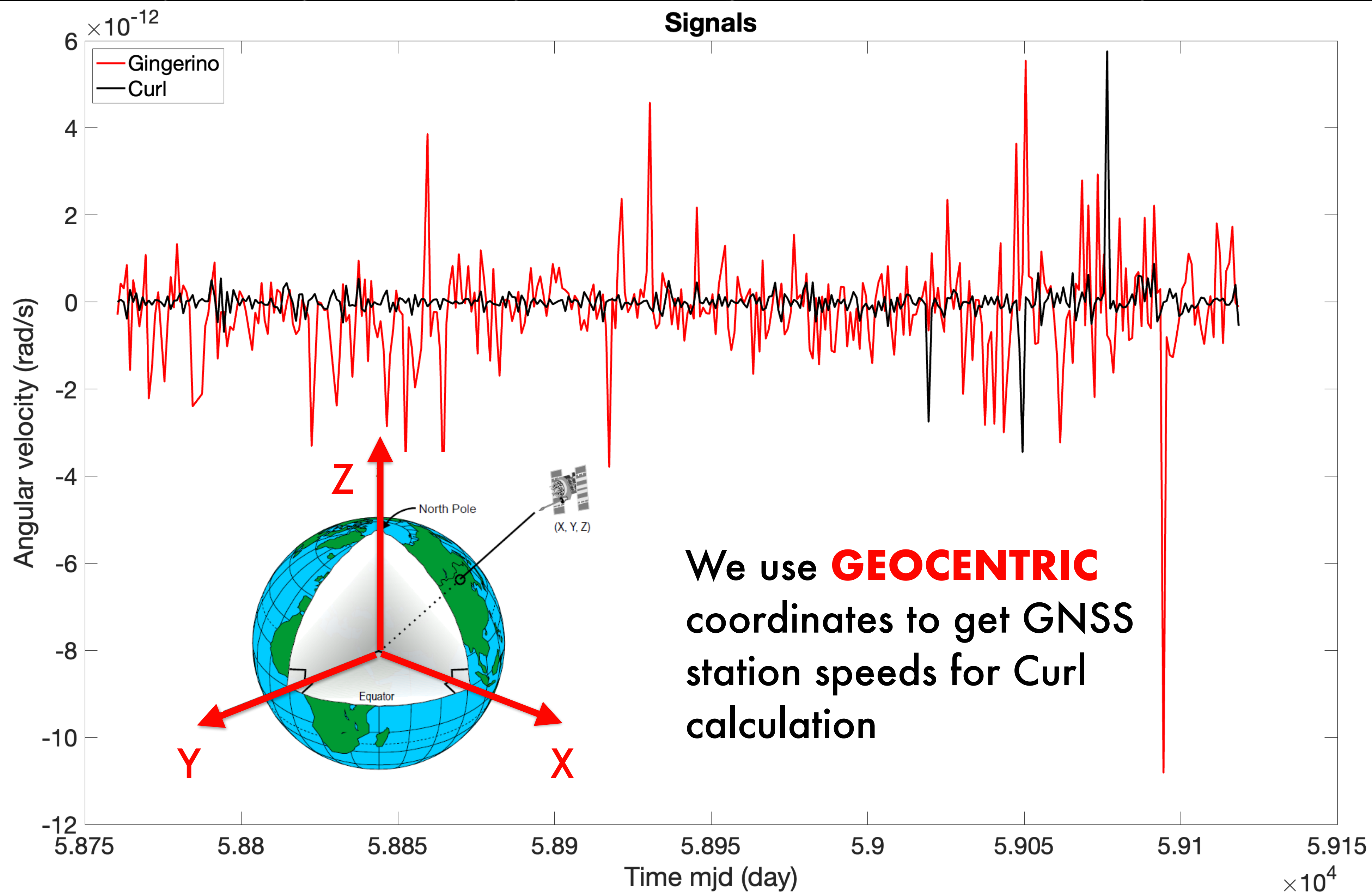
[https://link.springer.com/
article/10.1140/epjp/
s13360-024-04960-3](https://link.springer.com/article/10.1140/epjp/s13360-024-04960-3)

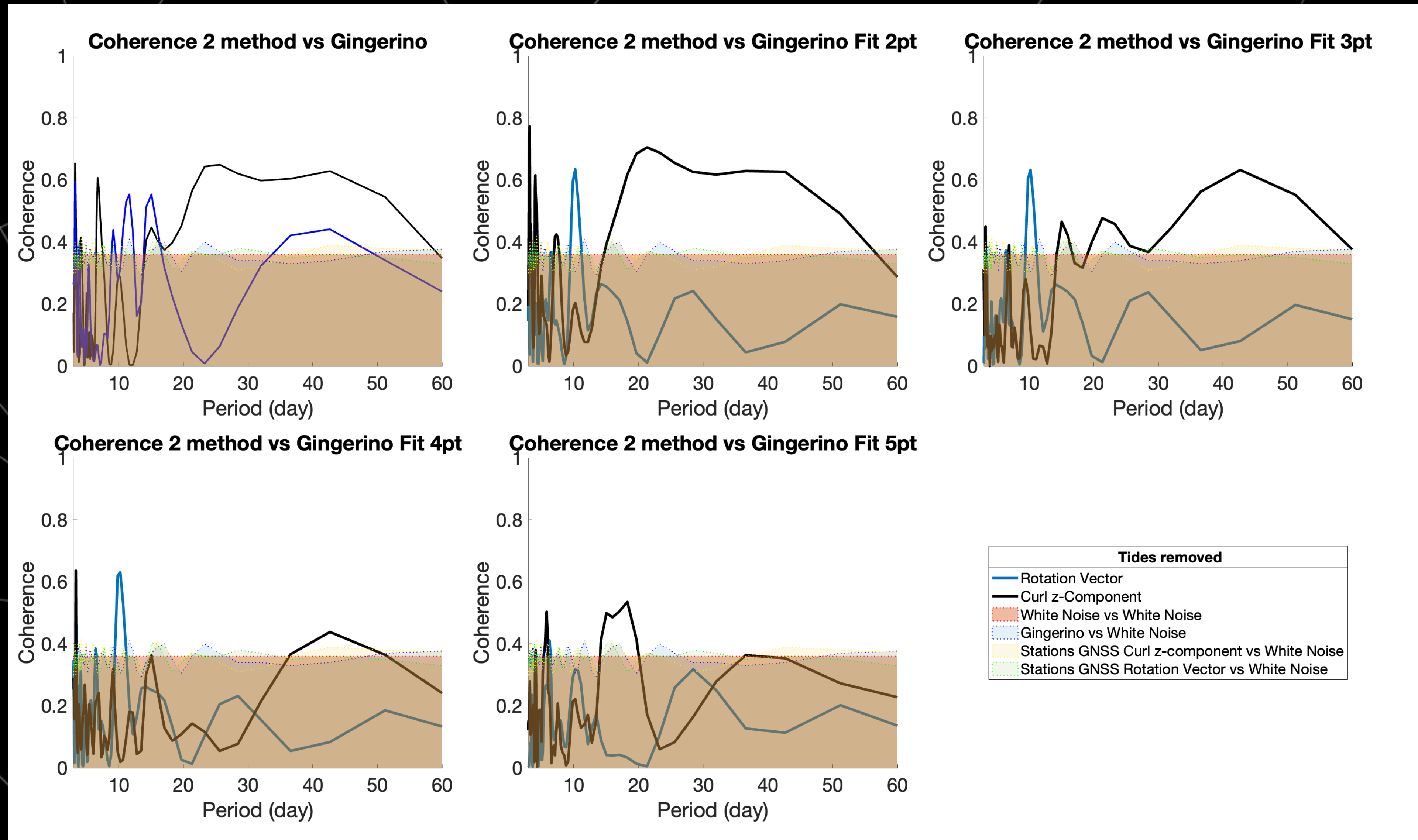
Rotational component from GNSS stations



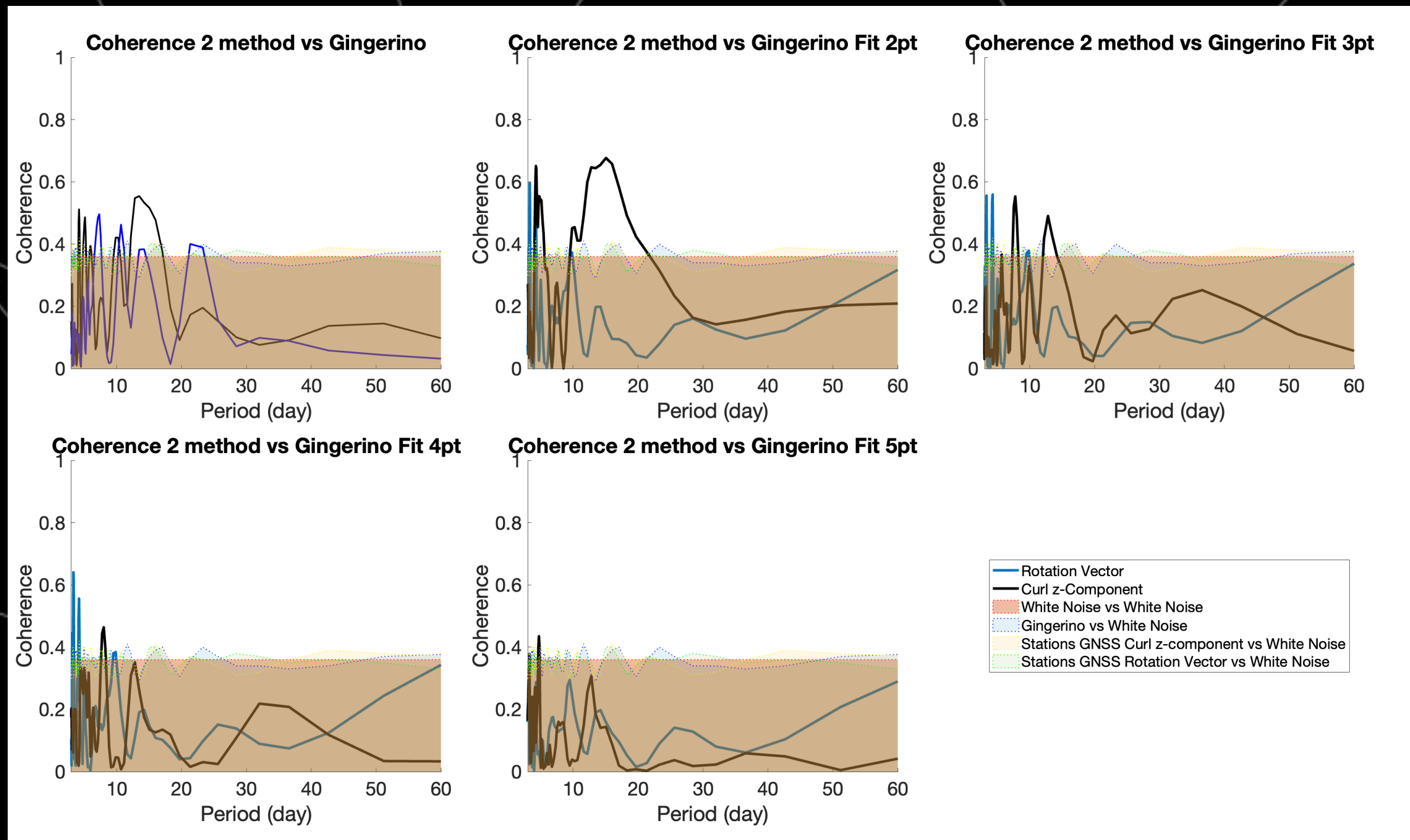
Curl z-component seen from GNSS stations

4

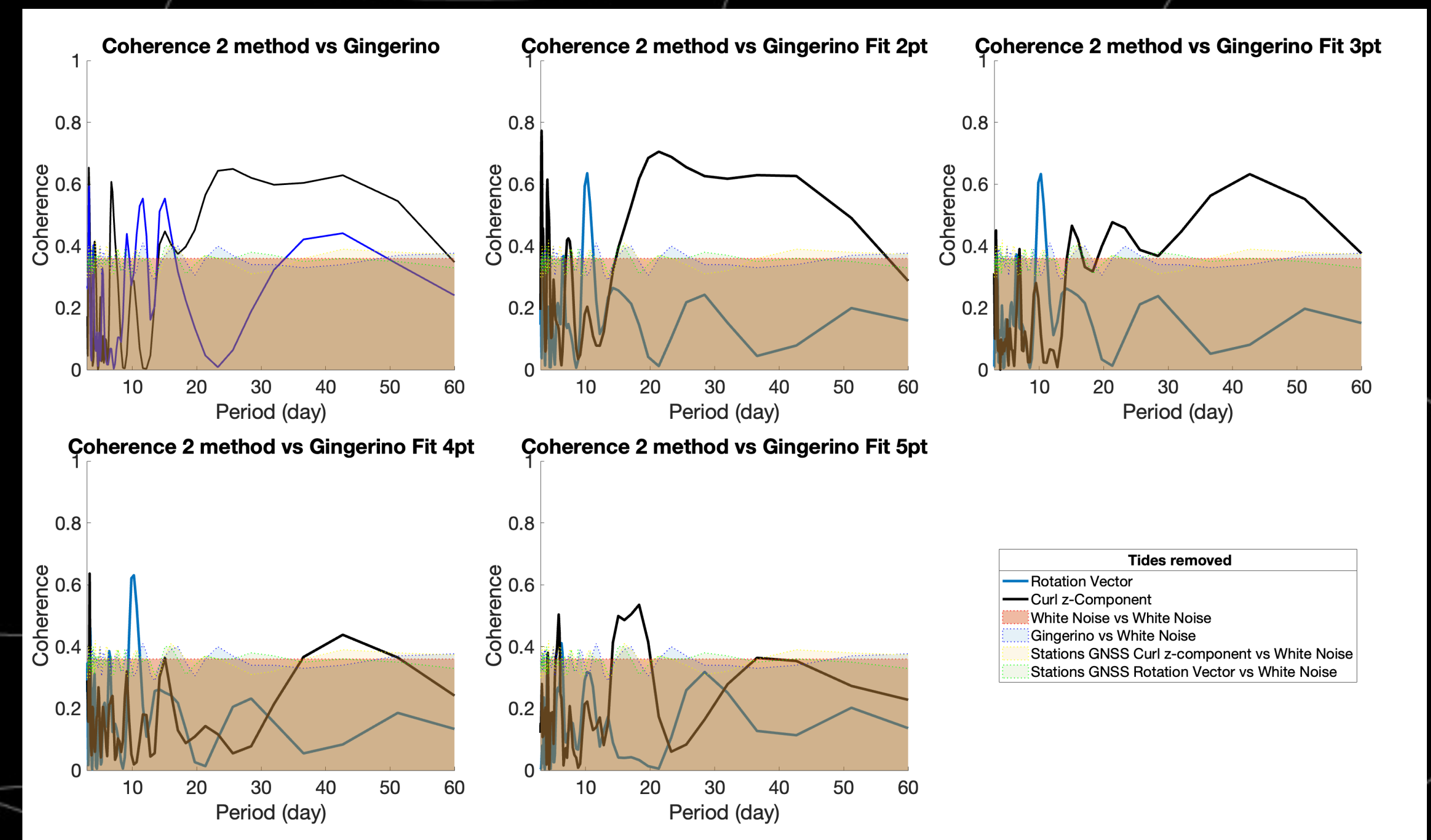




Fit of linear velocities



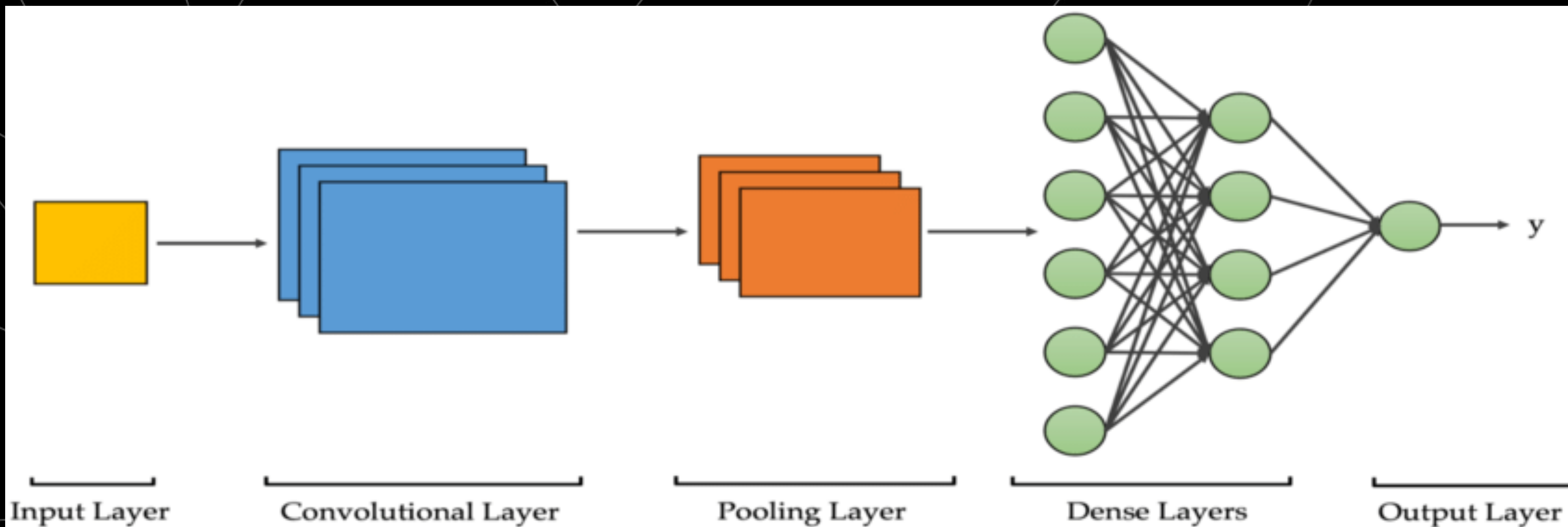
Coherence obtained without subtracting the contribution of the tides, clear structures emerge with the 2-point fit, these are decreasing for multi-point fit because the statistics decrease and the signals obtained go under the noise of the Gingerino signal.



Coherence achieved through the resolution of tides in Gingerino. In this case, the usual tidal peaks are reduced, revealing previously hidden structures with periods exceeding 20 days.

TCN and correlations

7



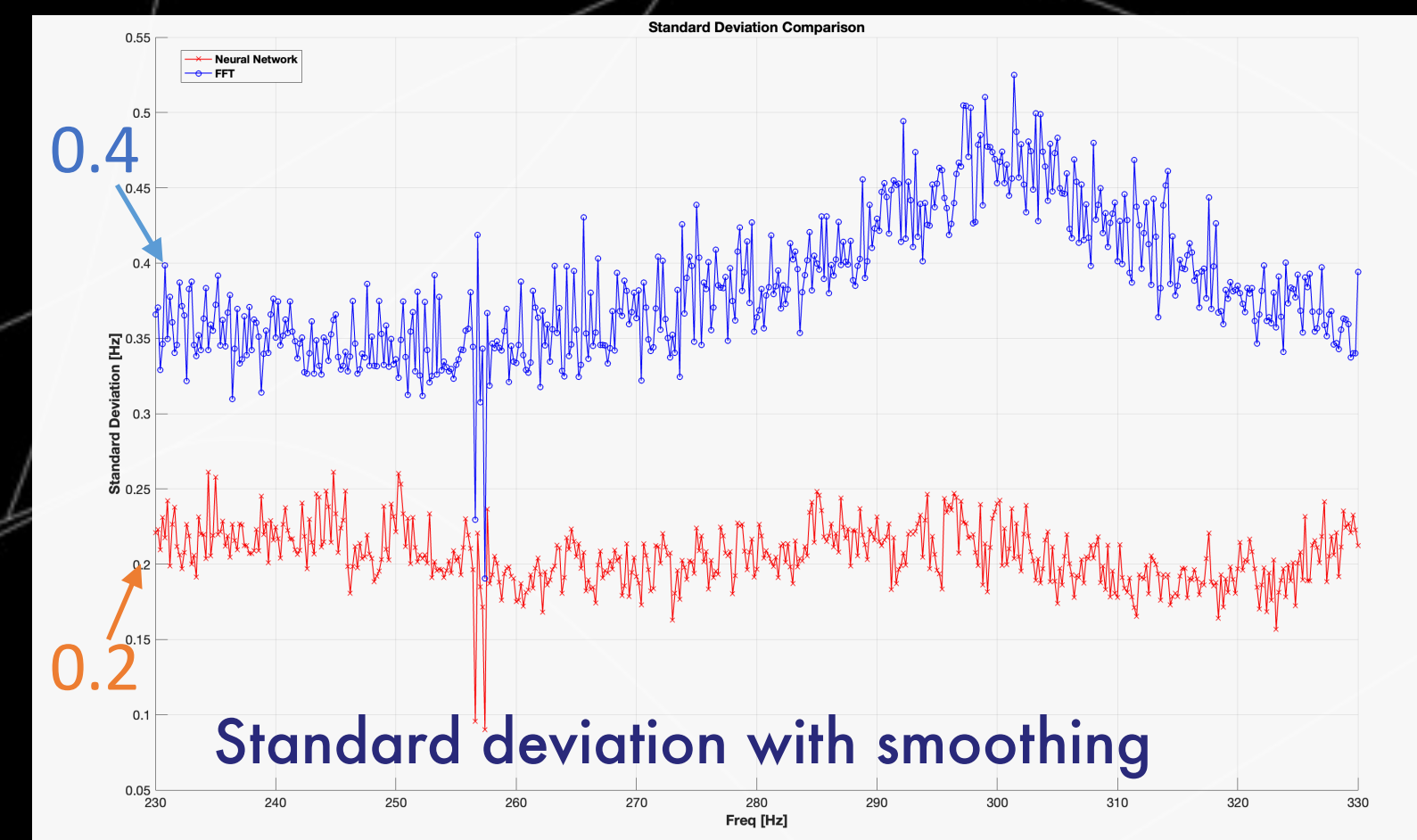
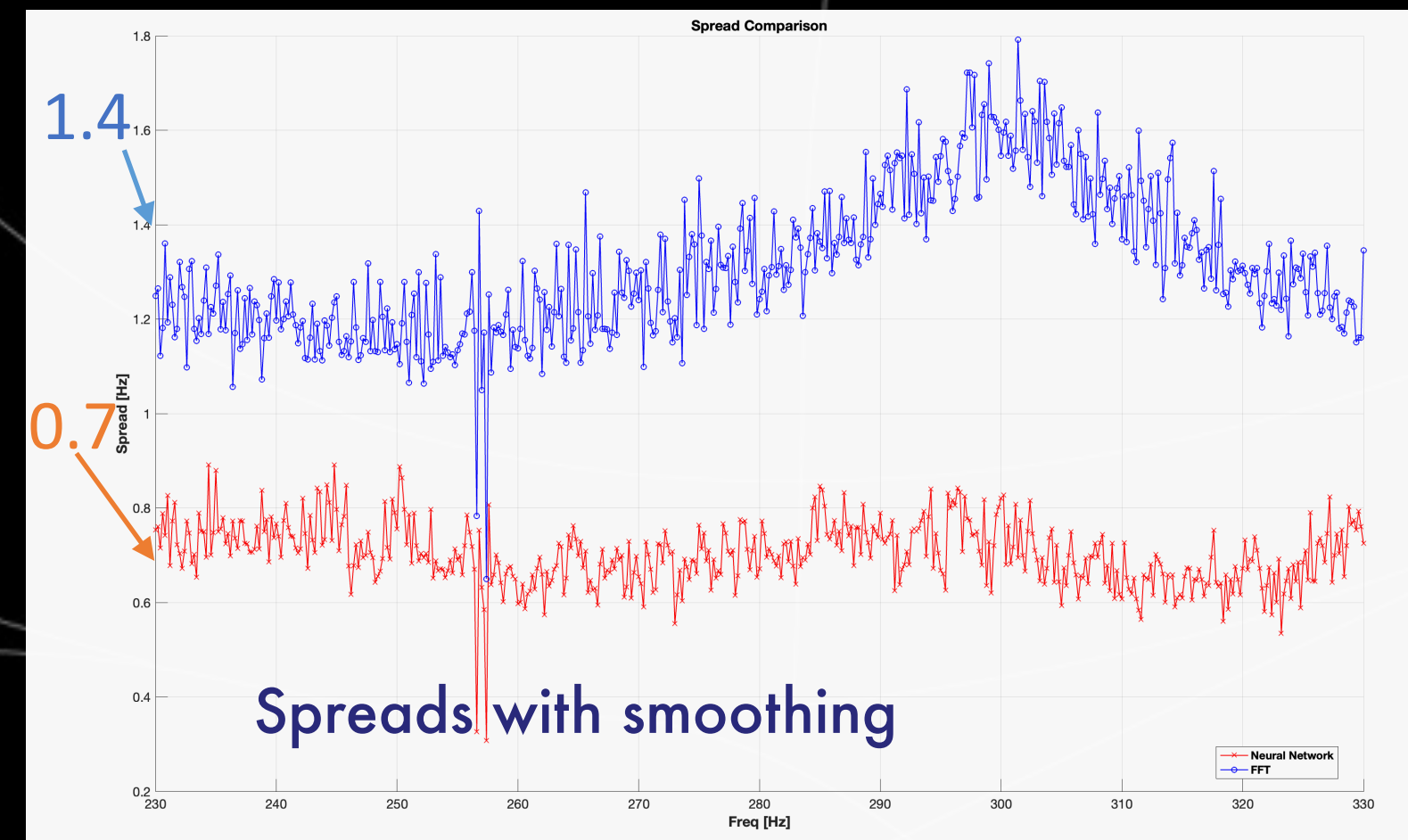
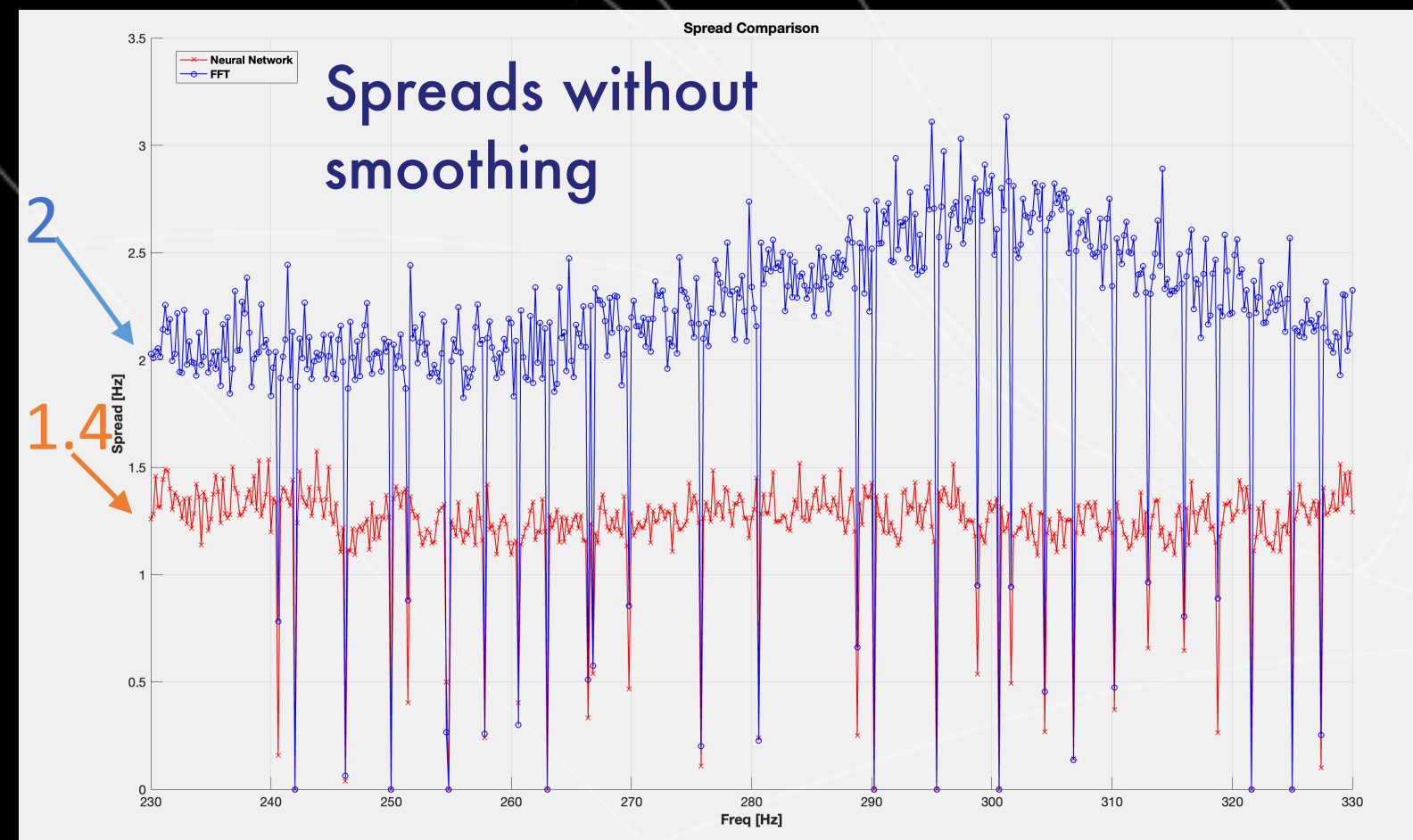
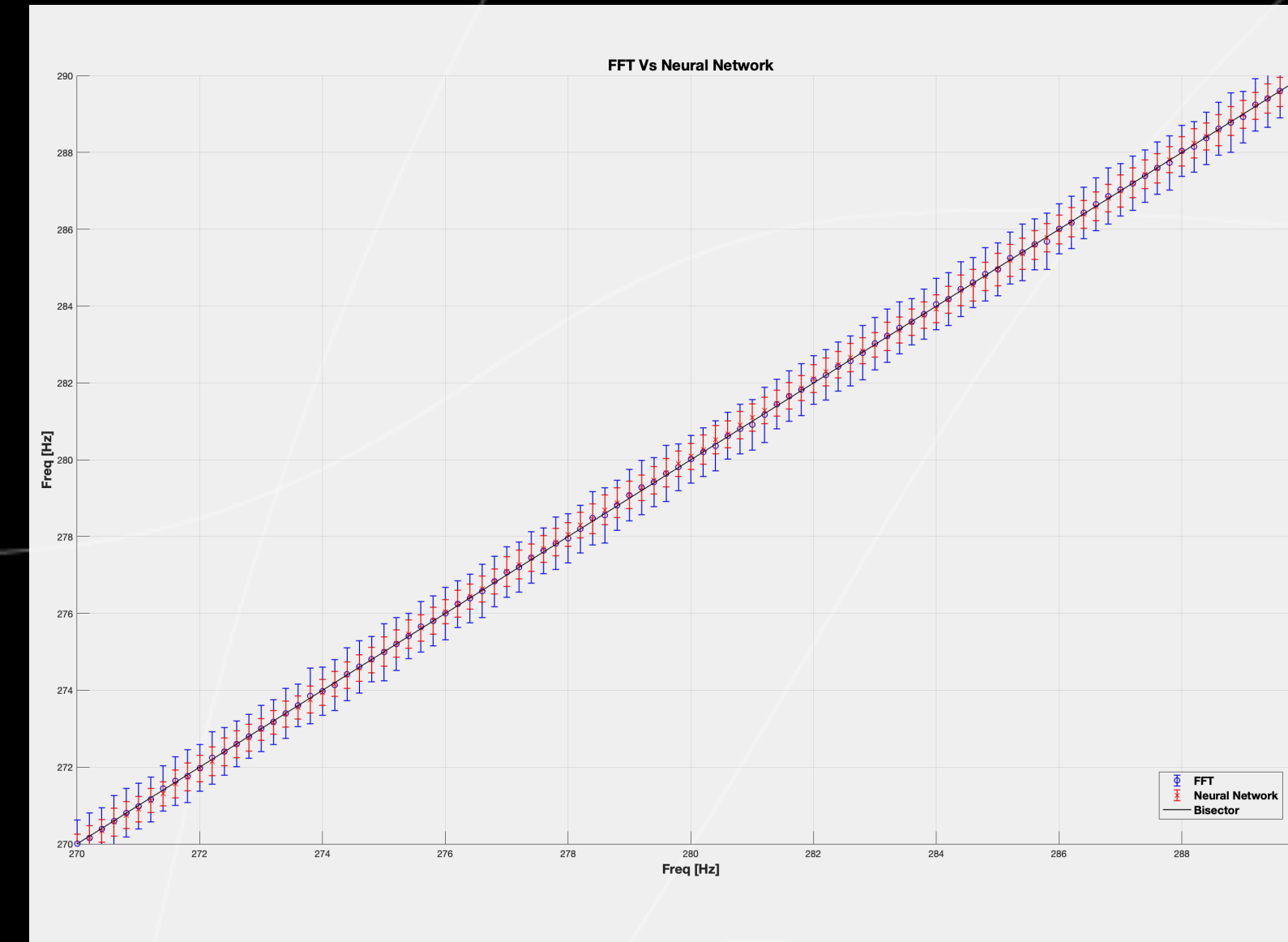
We used synthetic sinusoids with different frequencies and starting phases; we also varied their amplitude and mean value, or adding Gaussian noise to avoid overfitting; since the real signal always has the same average frequency, the network memorizes without generalizing and loses its robustness. Additionally, the network that achieved the best results was the one that output both the frequency and the cleaned sinusoid. This strategy ensures that by reconstructing both the clean sinusoid and the frequency, the network learns to better correlate the two pieces of information.

Testing on signals at different frequencies

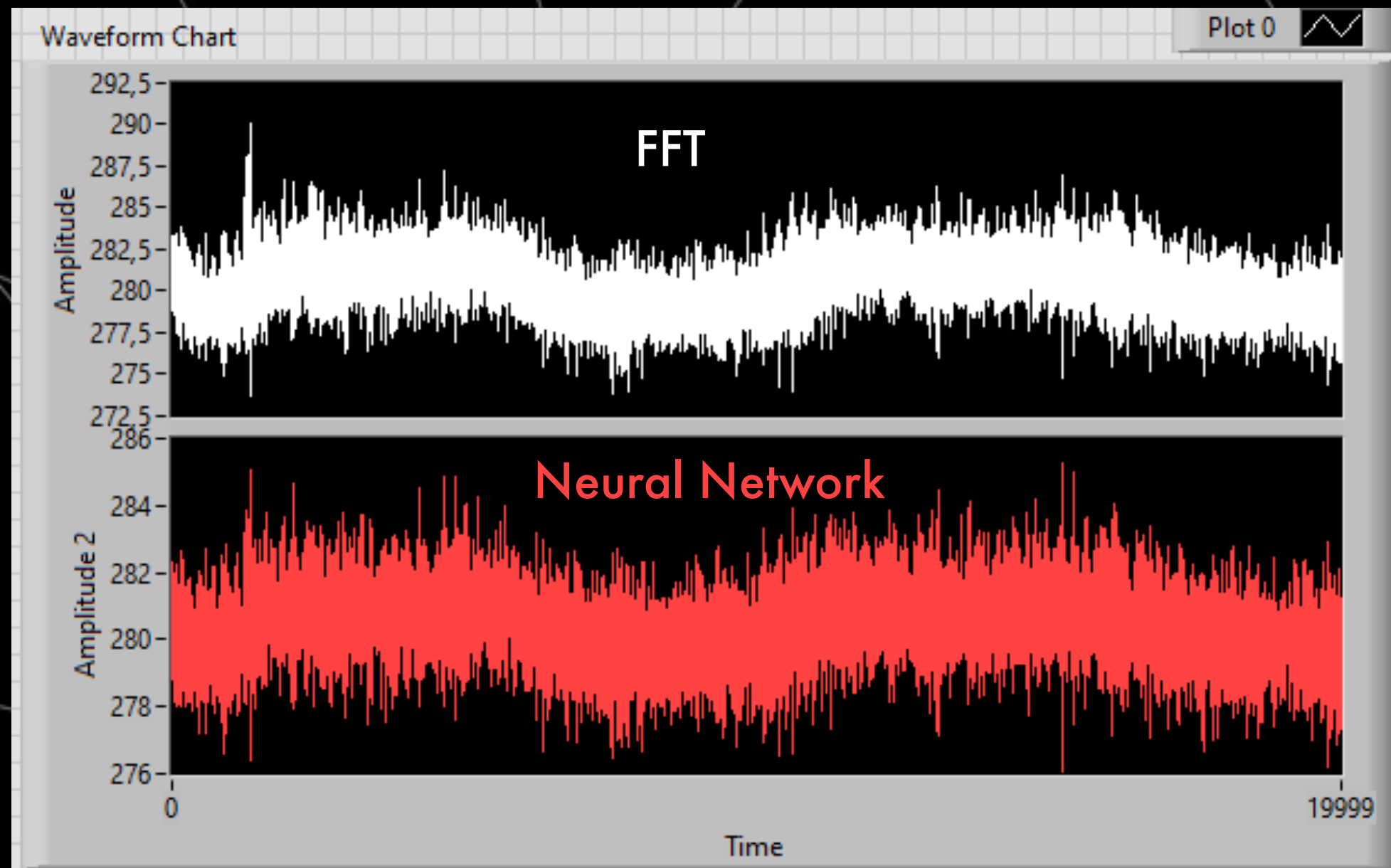
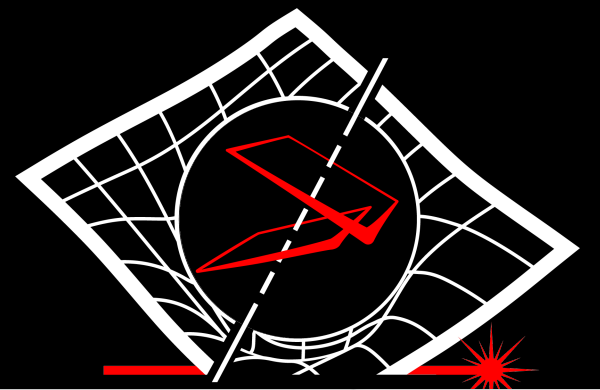
8



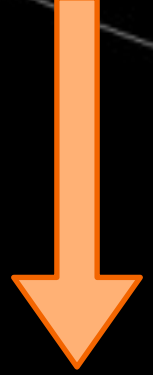
We compared this NN with a tool implemented in Labview based on FFT. We applied these two methods to recover frequency from simulated signal with Gaussian noise and a frequency range between 150 Hz and 350 Hz. Across the entire range, the NN is twice as accurate as the FFT in terms of both the standard deviation of the reconstructed frequency signal and the spread.



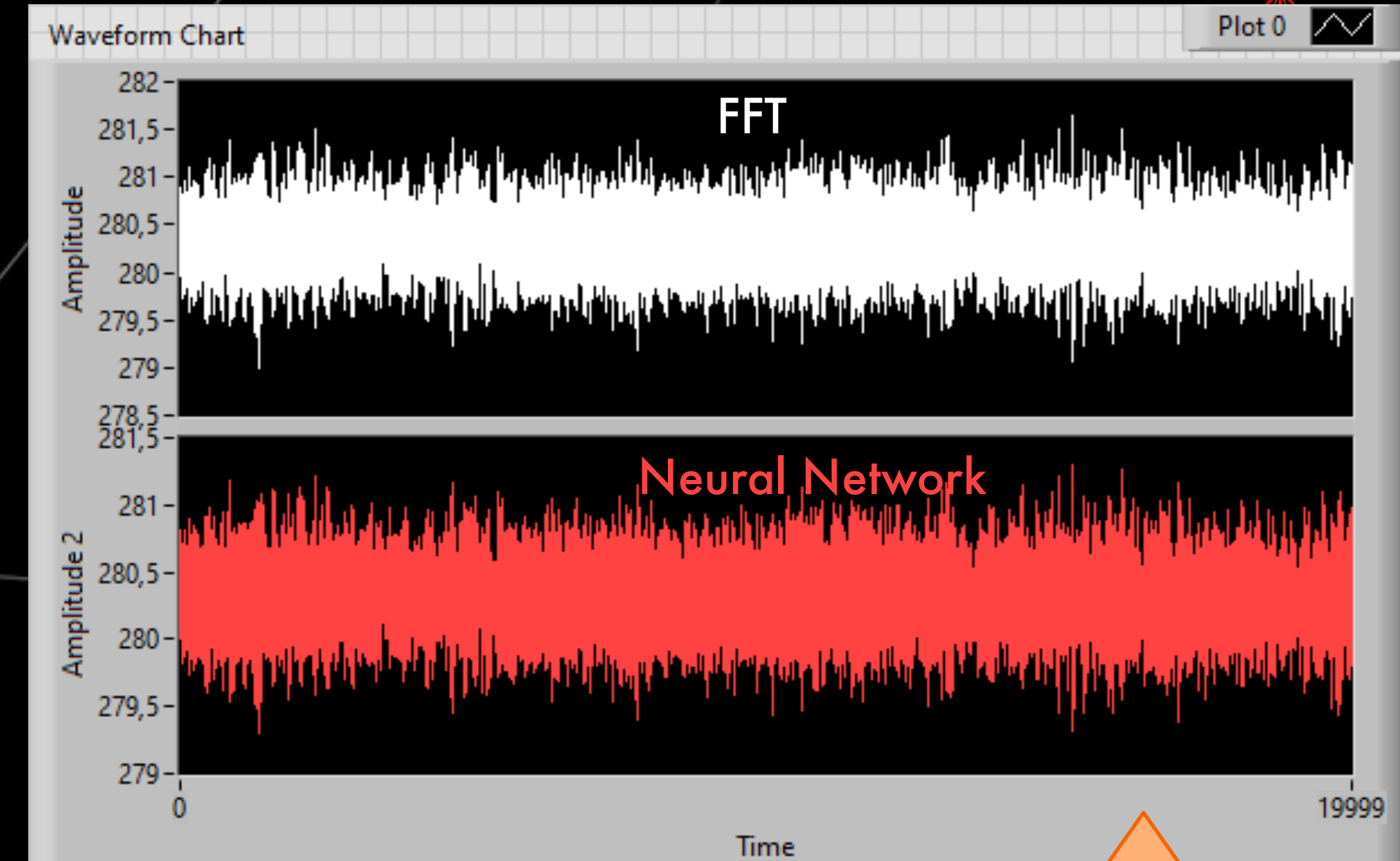
Testing on real-signal



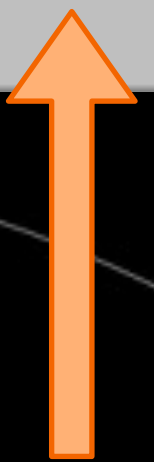
Spread: 6.8 Hz
 σ : 2.0 Hz
Spread: 3.5 Hz
 σ : 1.0 Hz



Smoothing

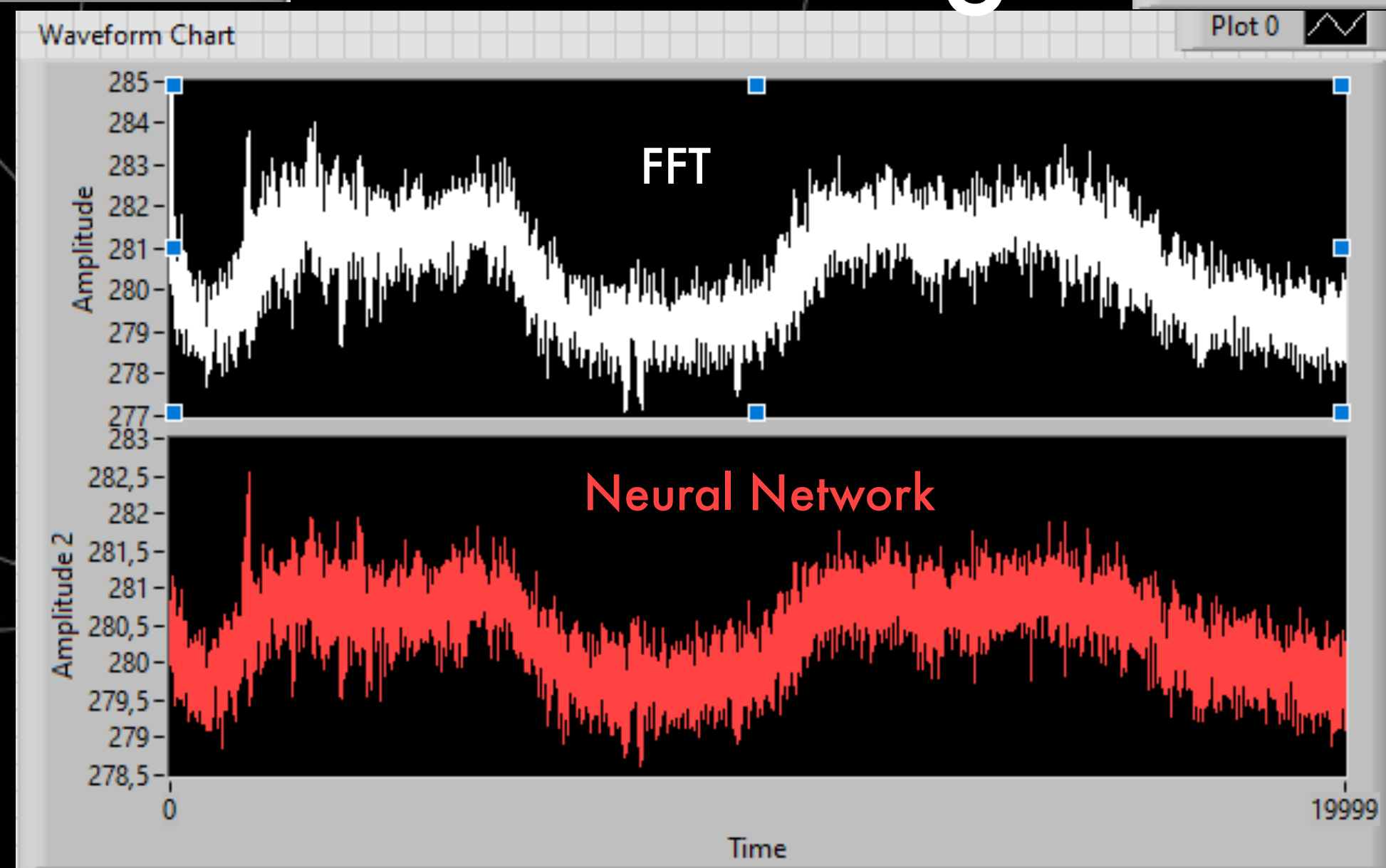


Filter



Spread: 2.6 Hz
 σ : 0.8 Hz
Spread: 2.0 Hz
 σ : 0.6 Hz

Spread: 16.2 Hz
 σ : 4.7 Hz
Spread: 9.1 Hz
 σ : 2.7 Hz

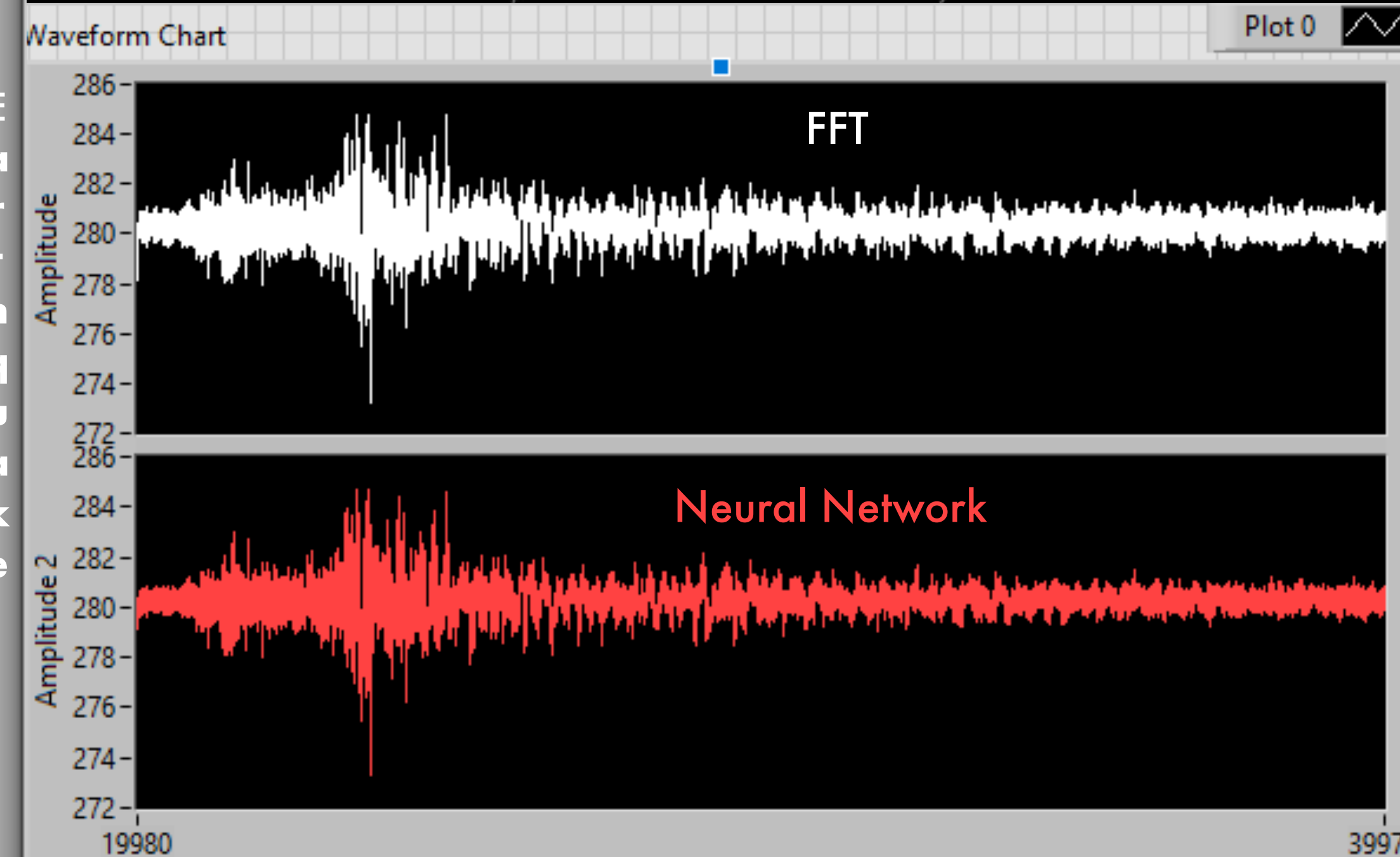
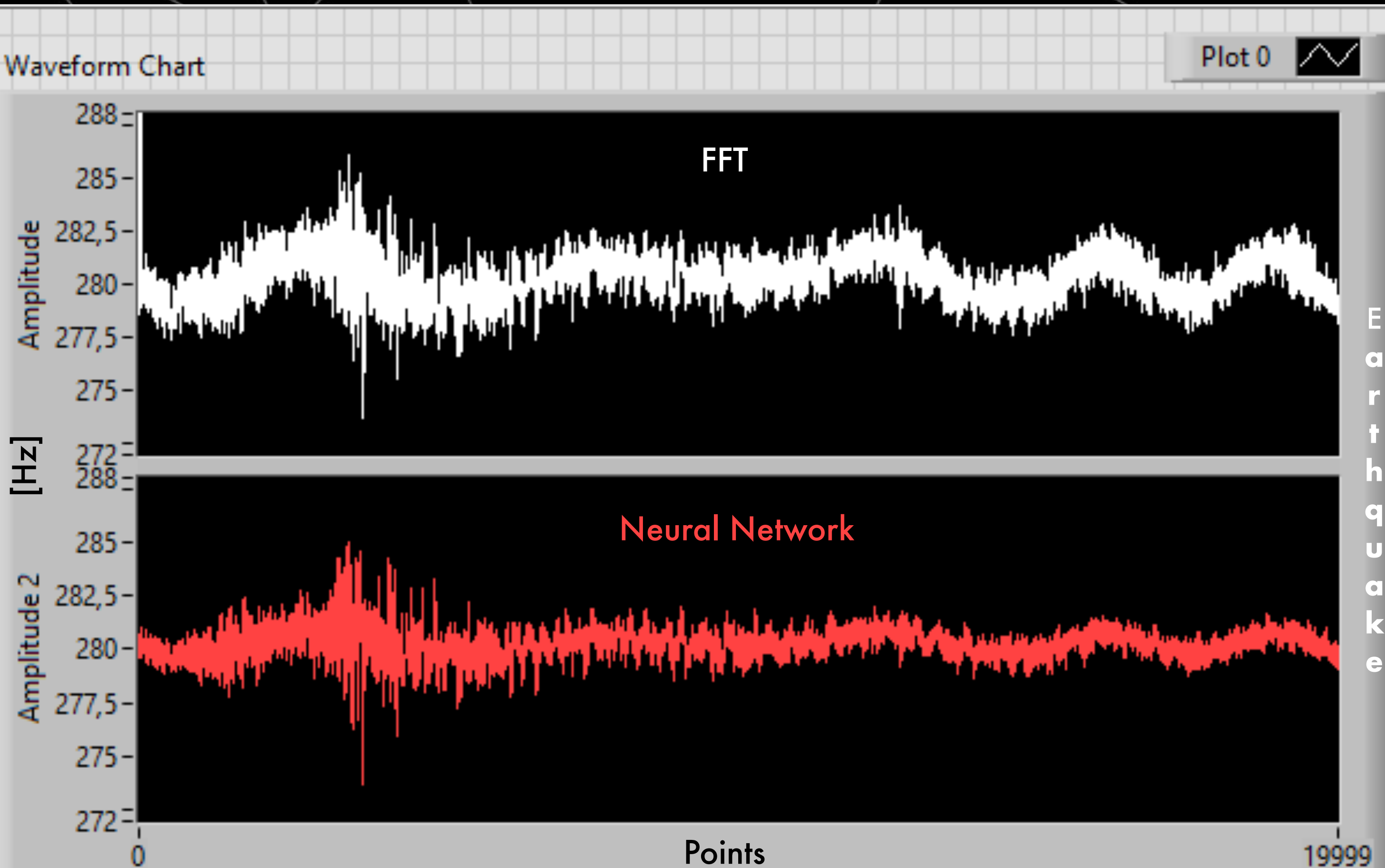


Test on an earthquake signal

10



By comparison of the NN with the FFT on a real signal we can see that it does not eliminate or depress part of the signal but reduces the effects of low-frequency spurious signals (Completely deleted using a Filter), thus improving the noise signal ratio.

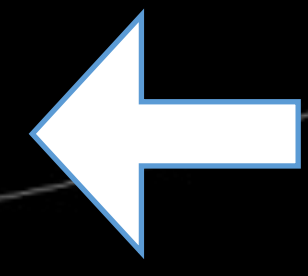
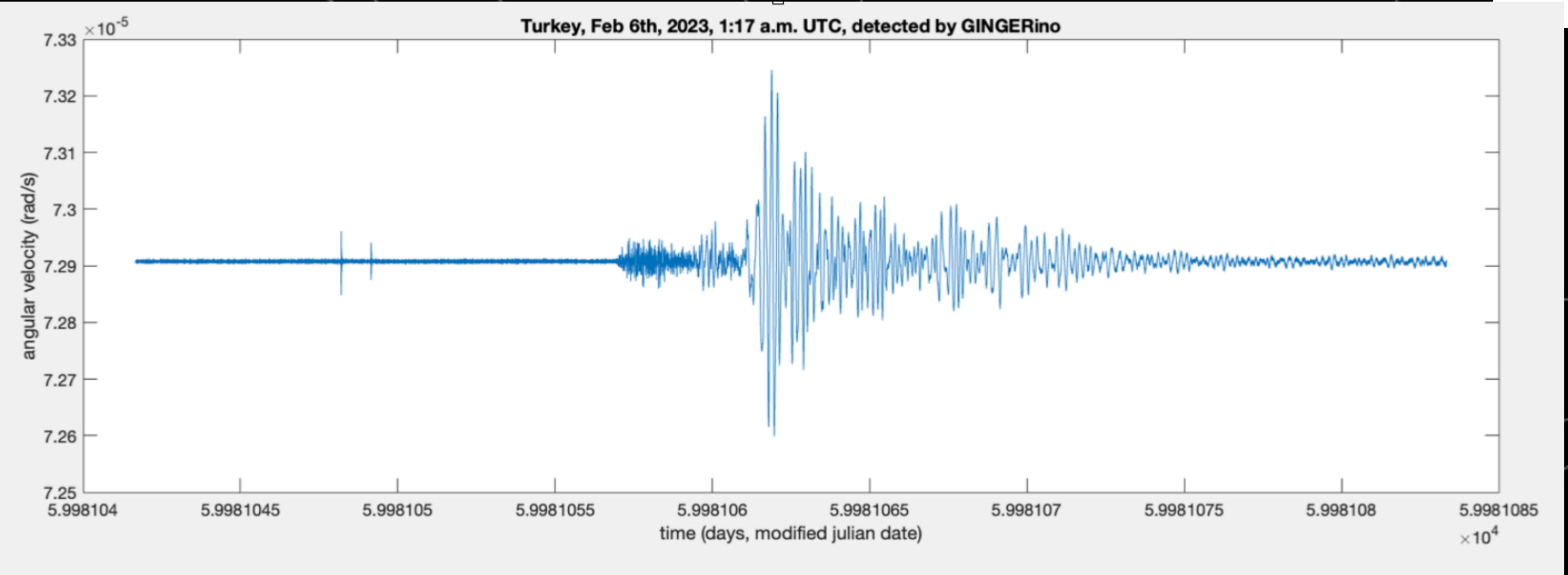
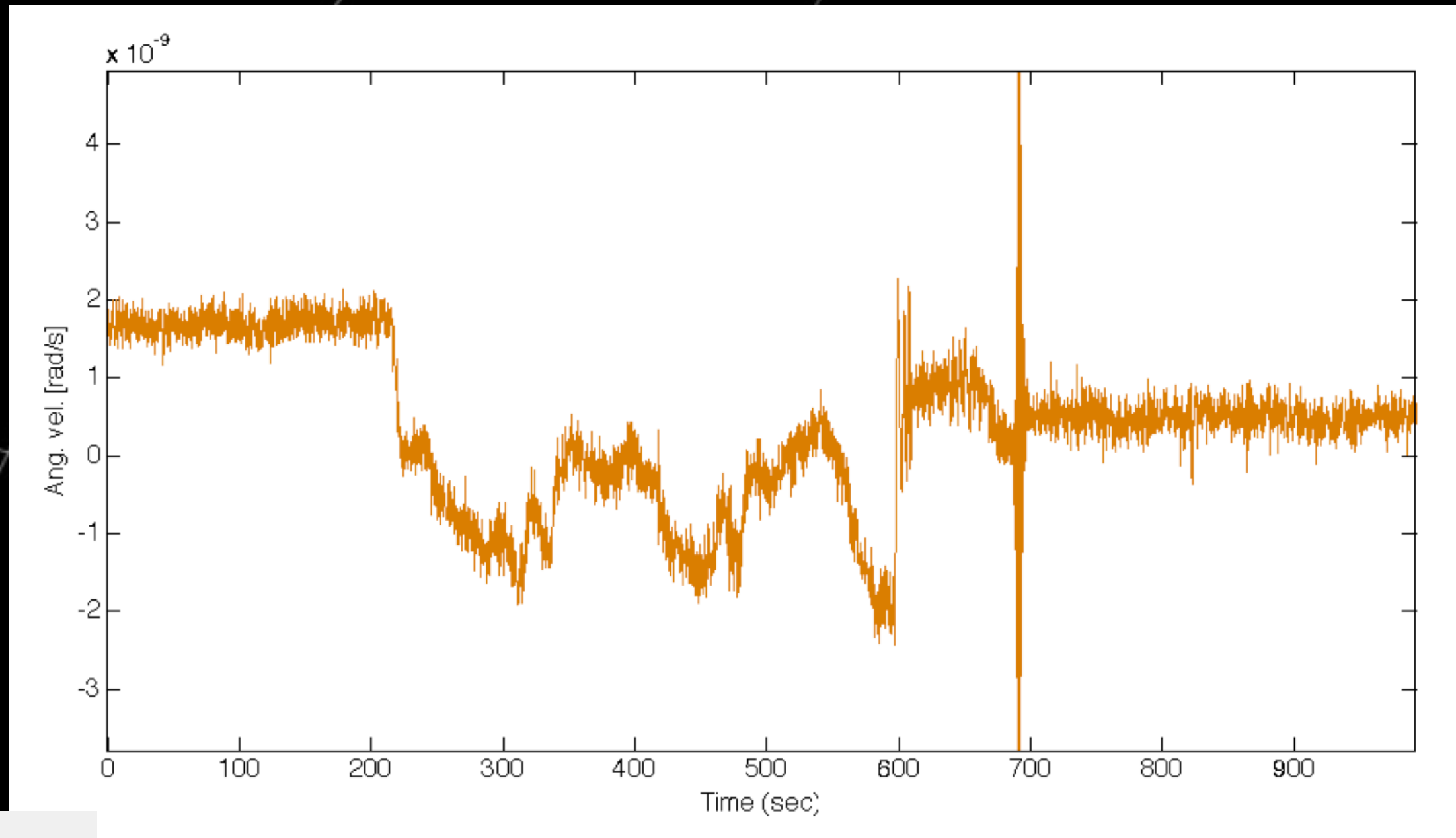
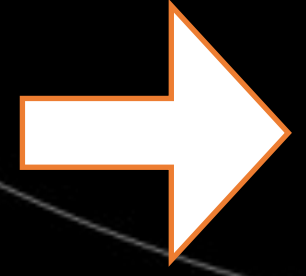


Filter

The typical disturbances of the reconstructed signal



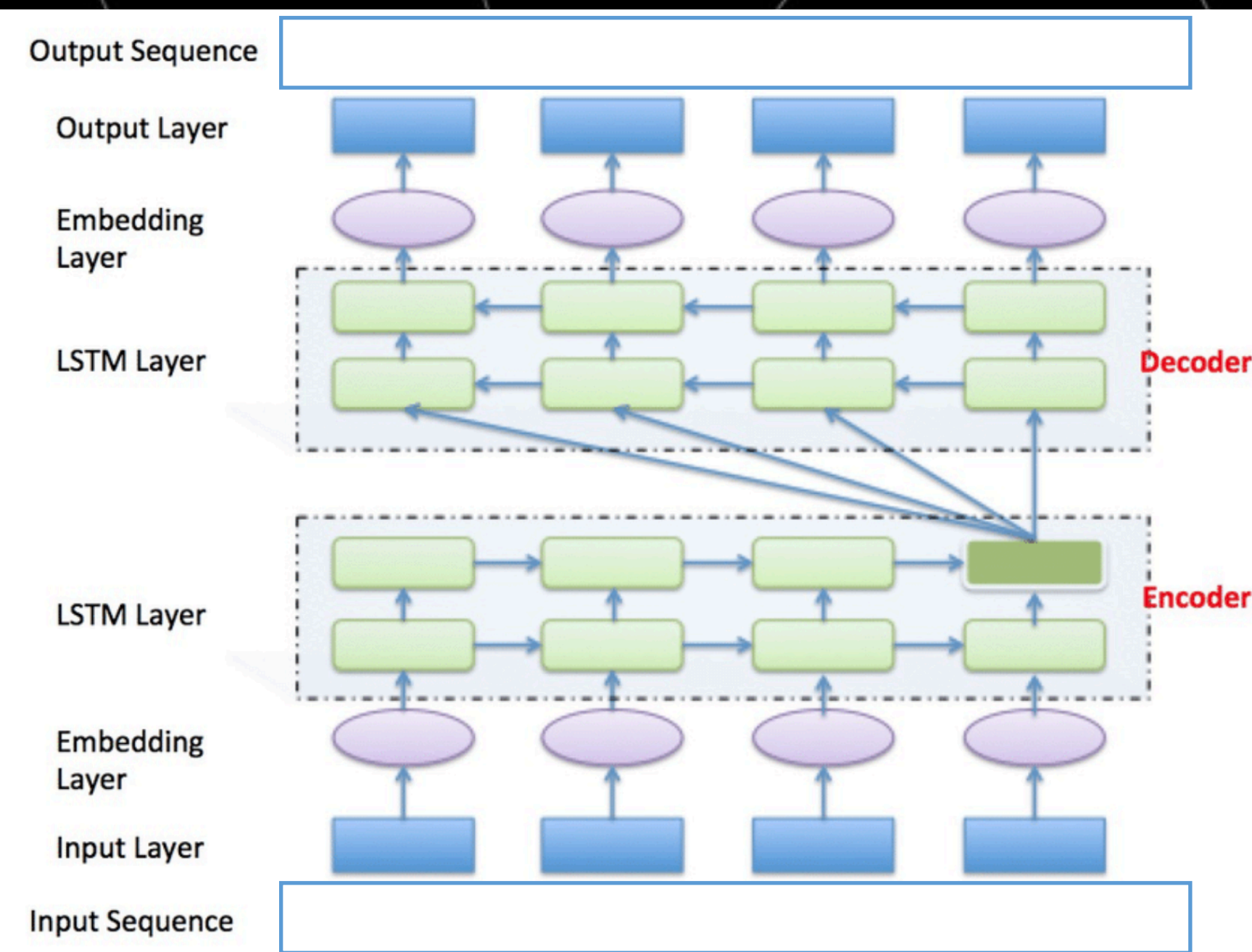
Typical disturbance due to laser dynamics during the mode jump



Contribution of the earthquake of Turkey of February 6th

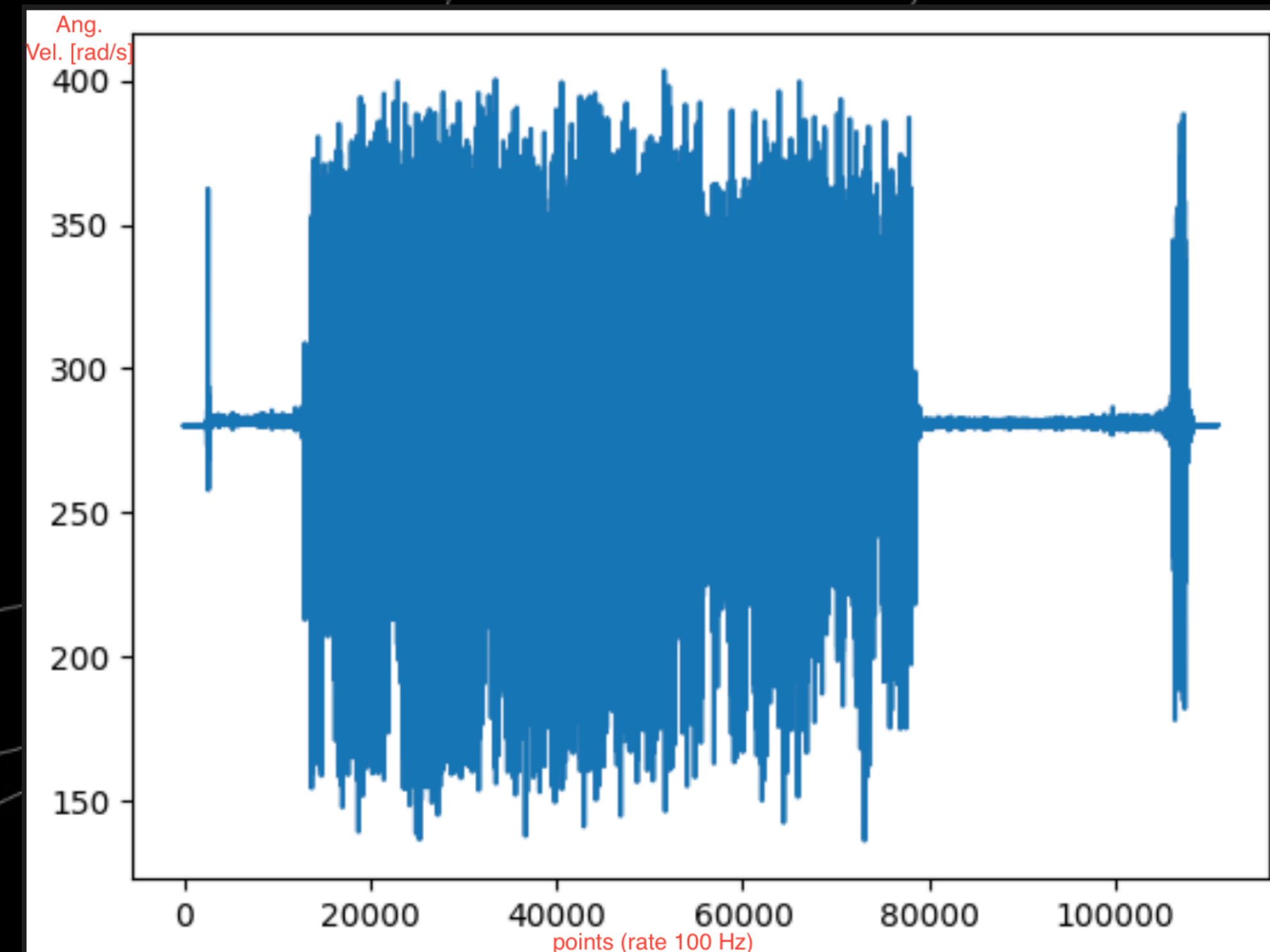
Structure of the NN classifiers

12



Although GINGERINO already has systems to classify the goodness of the signal and currently has a duty cycle of more than 90%, we are building NNs that identify disturbances from the laser. To do this we have as input the time series containing these disturbances and as output the mask that distinguishes between: 0 the good signal and 1 the anomalies. It might seem like a classification problem instead it is a regression problem, needing a seq2seq translator.

To create the dataset we have identified hours that present the various types of disturbances and divided into many pieces 6 seconds long at 100 Hz, to each of these we have then associated the mask that we then want to be returned by the neural network.

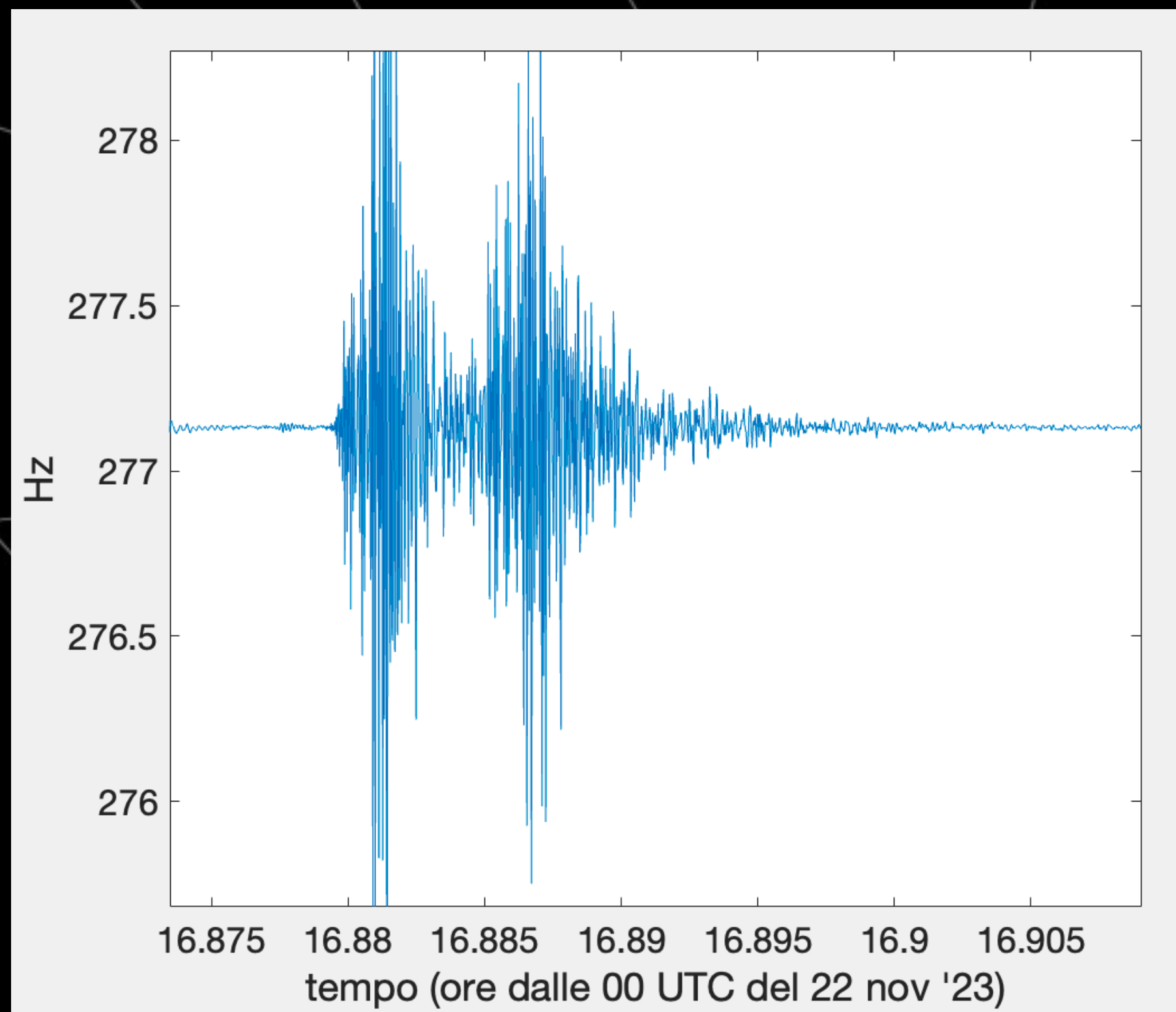


Map from GIGS to GINGERINO

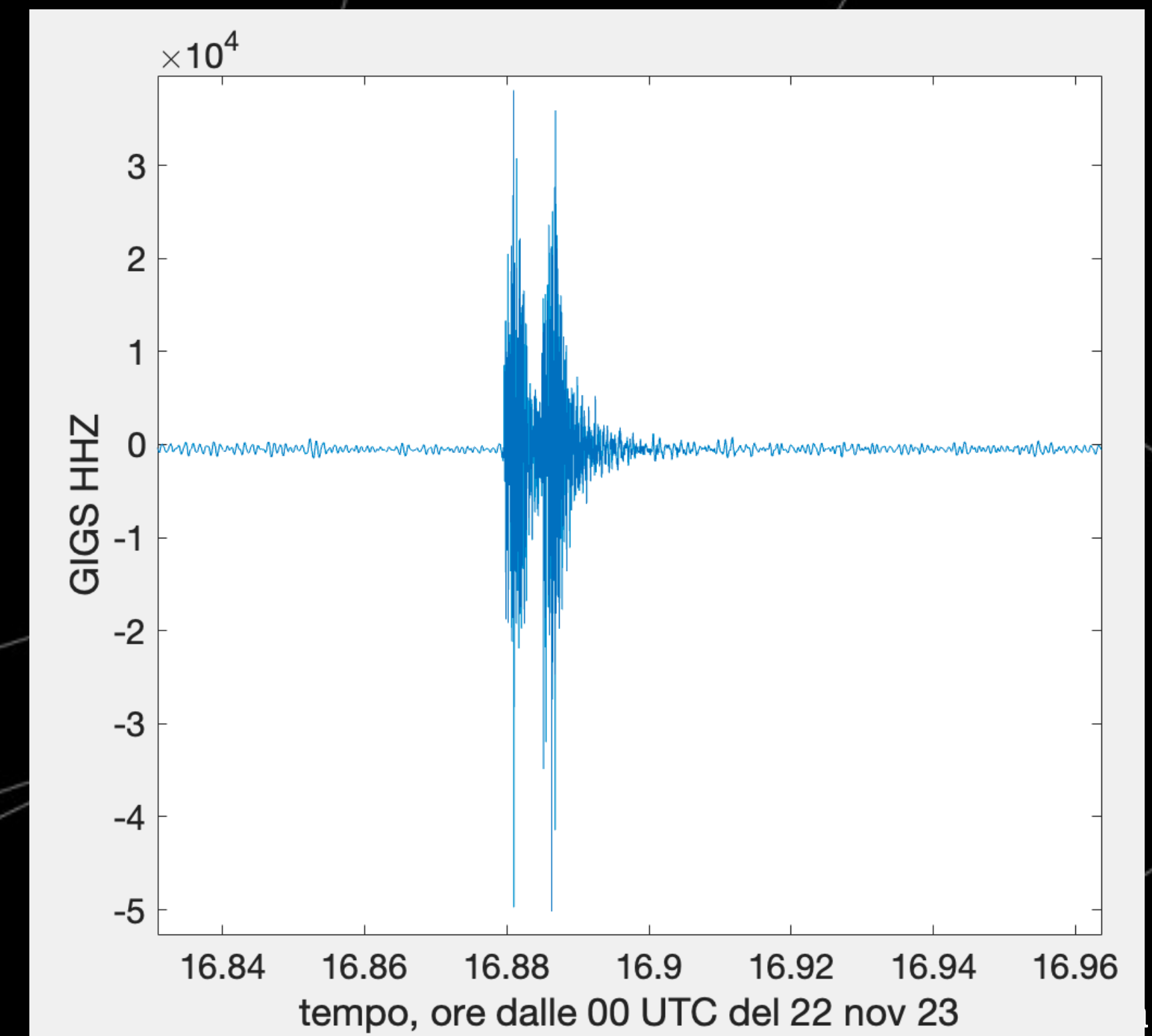
13



To have enough examples of earthquakes to train a network to recognize them, we create a network that generates the earthquakes seen by a Ring Laser Gyroscope (RLG), starting from the earthquakes revealed by GIGS. This is possible because we have a GIGS station co-located with GINGERINO. This NN is later applied to other stations similar to GIGS to obtain new examples of earthquakes seen by an RLG



Map from GIGS
to GINGERINO





**THANKS
FOR YOUR ATTENTION**

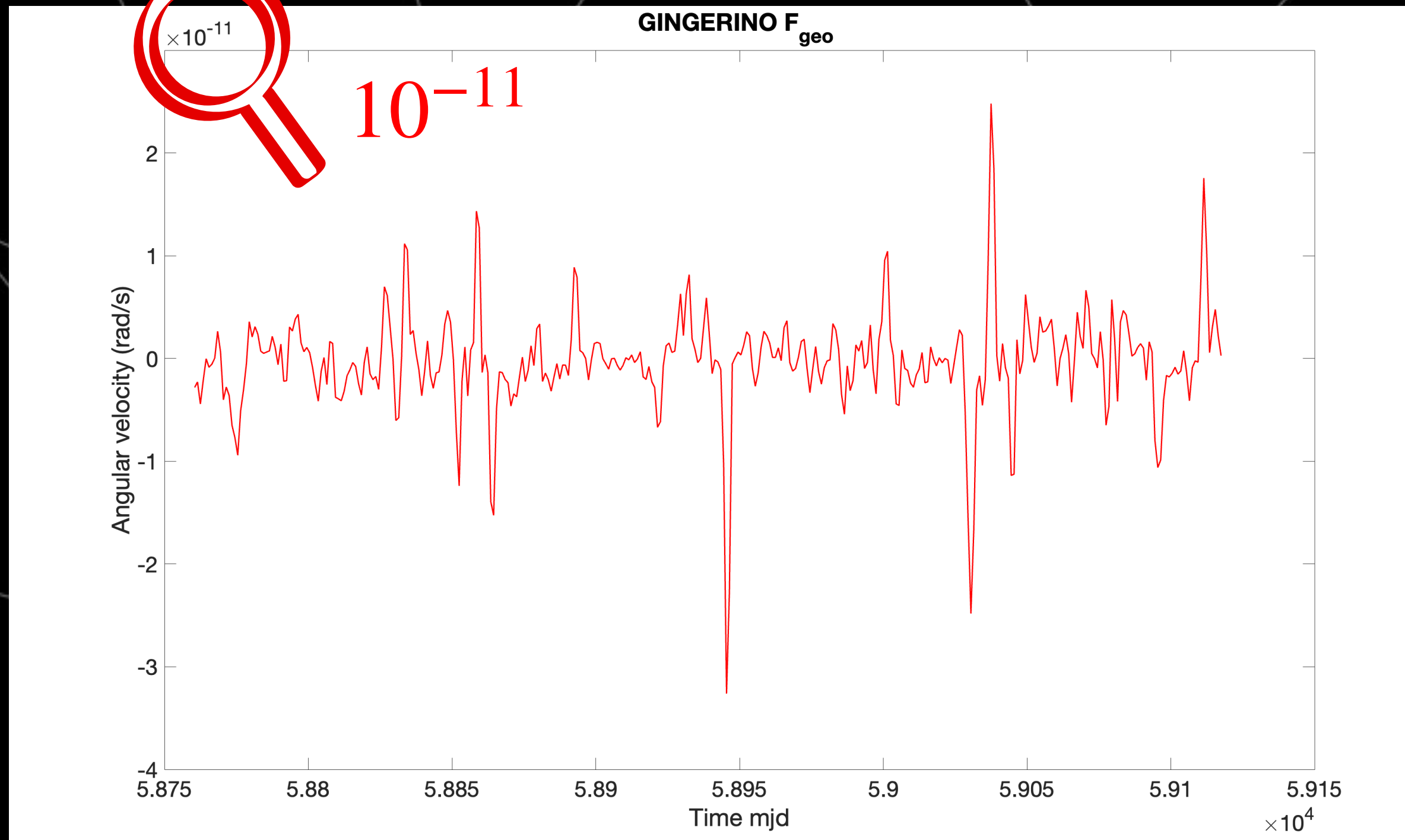


15

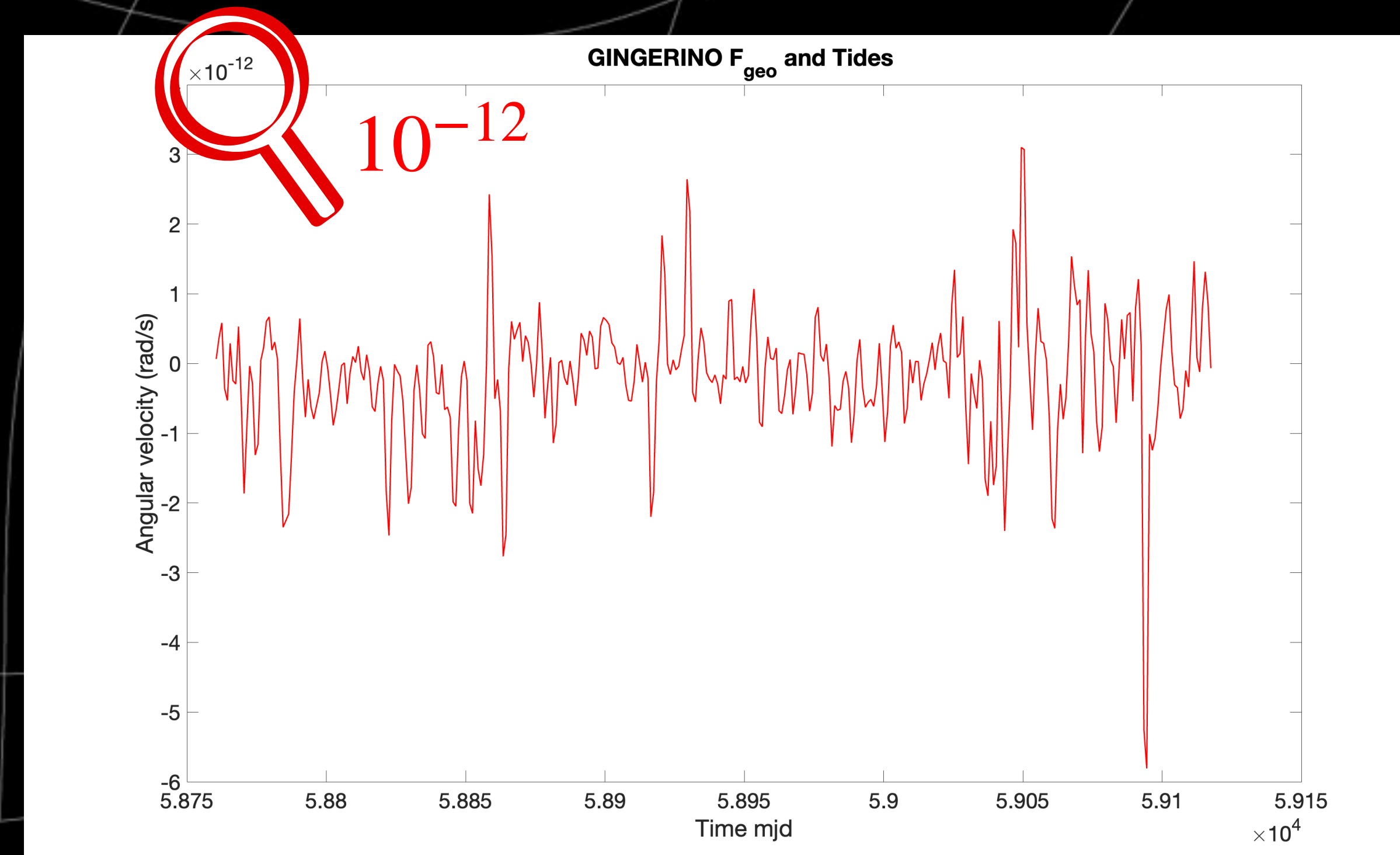


Gingerino Signals

16



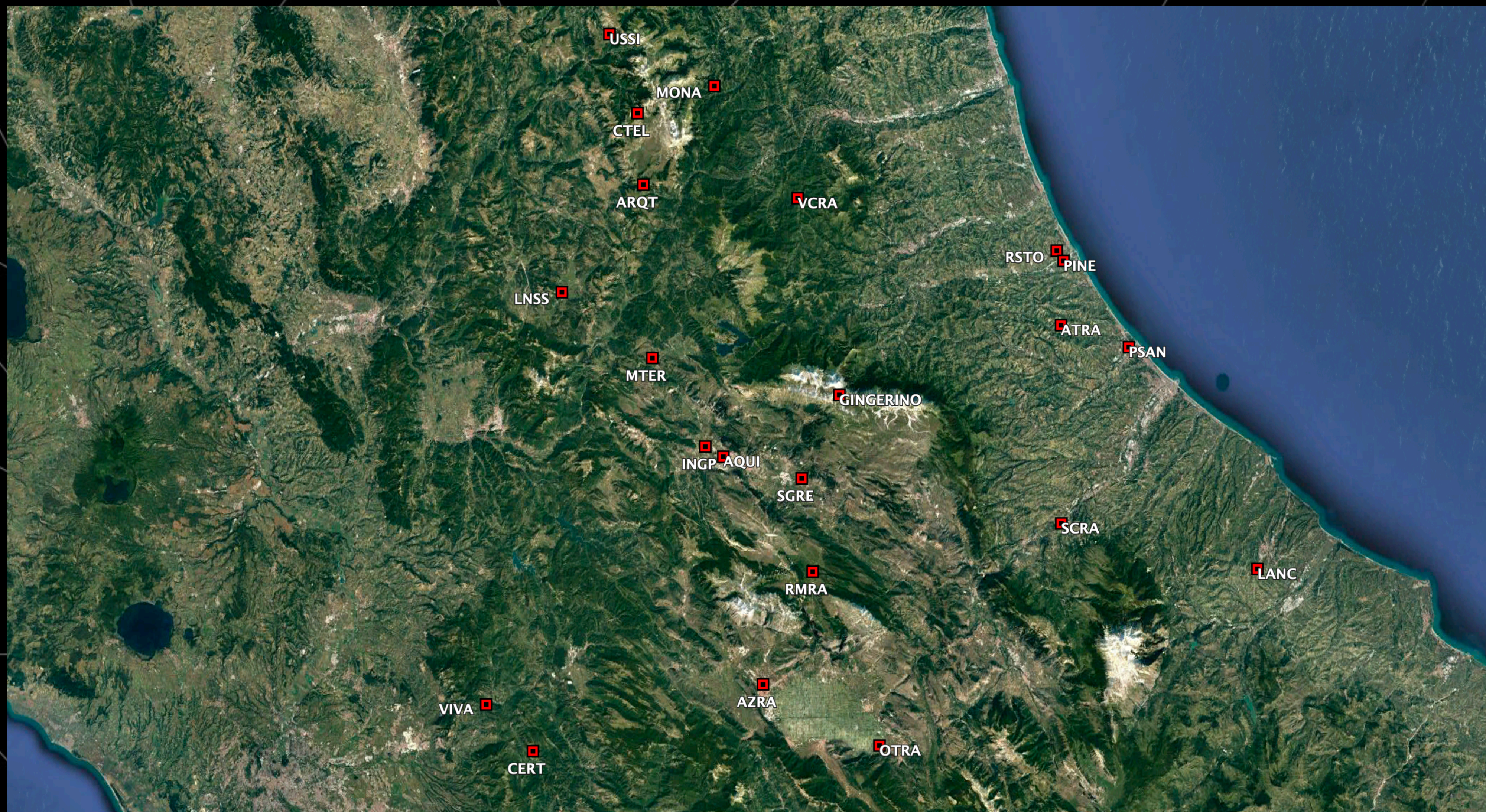
We have on the left the Gingerino signal in which systematic laser corrections and terrestrial rotational component, including polar motion and Chandler wobble (obtained from **IERS** measurements) were removed.



On the right we have the Gingerino signal, obtained starting from the previous one, in which we solved and subtracted the tides through the use of the **GOTIC2_mod** program [2].

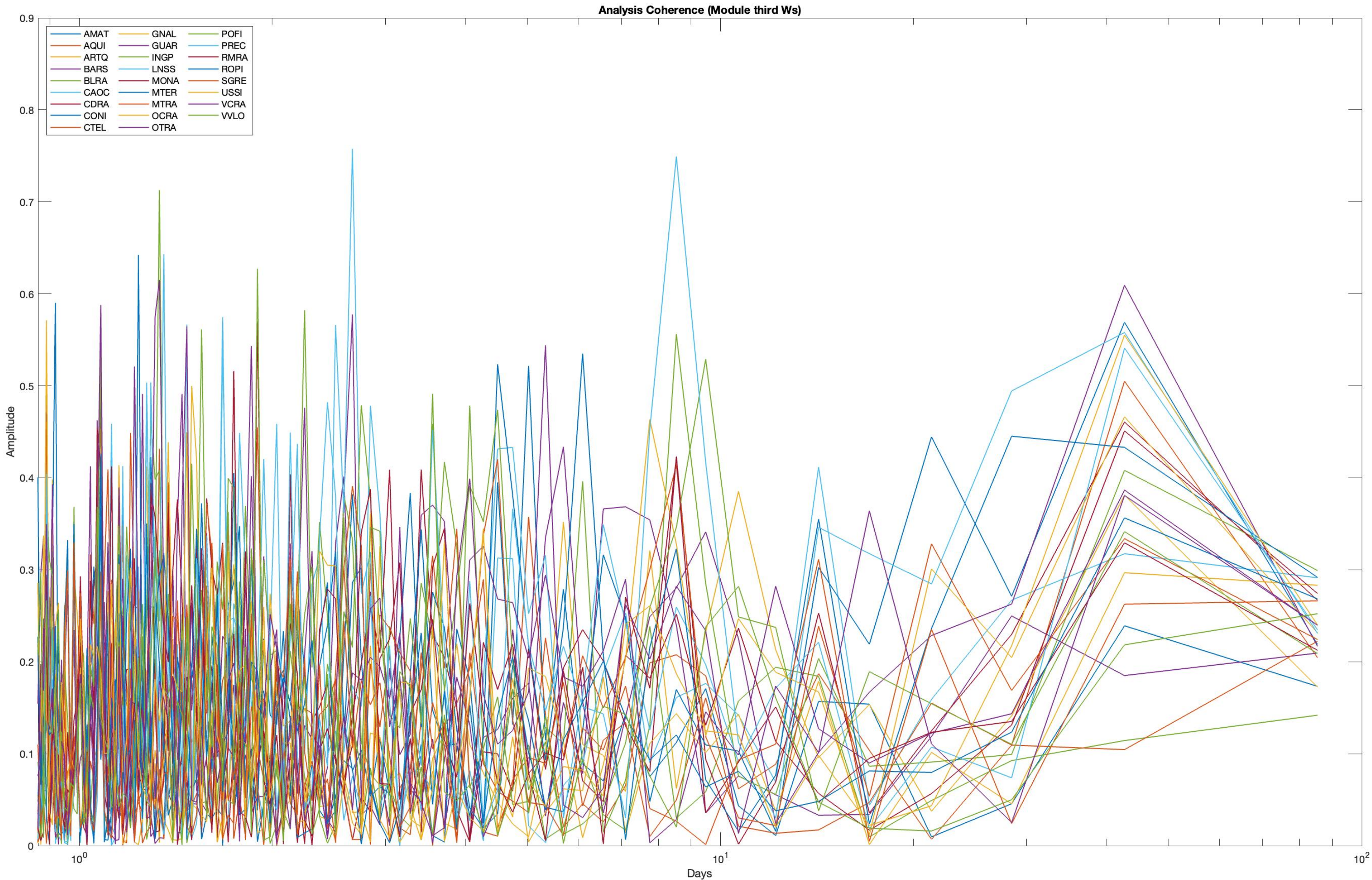
The constellation of GNSS stations

17



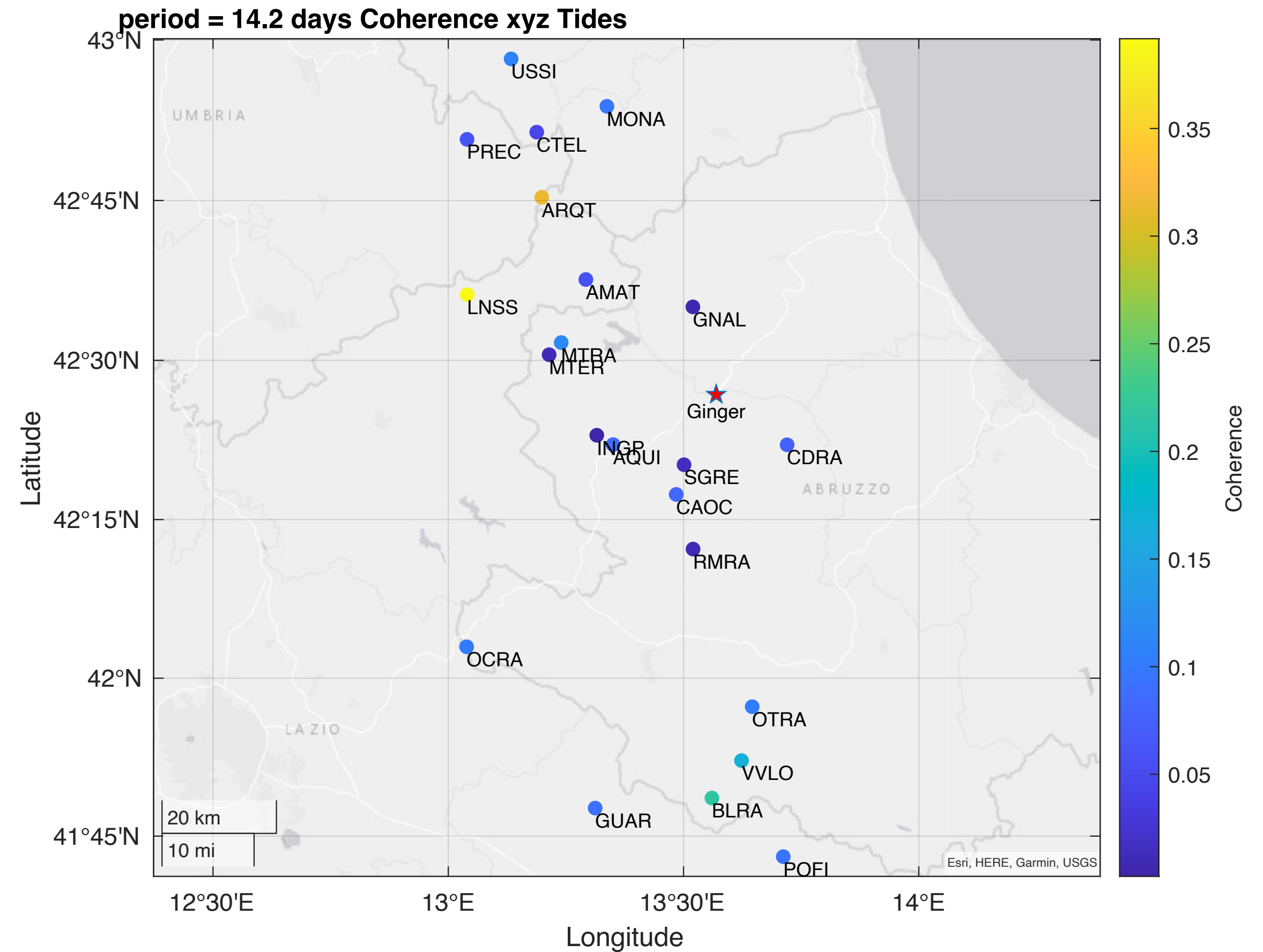
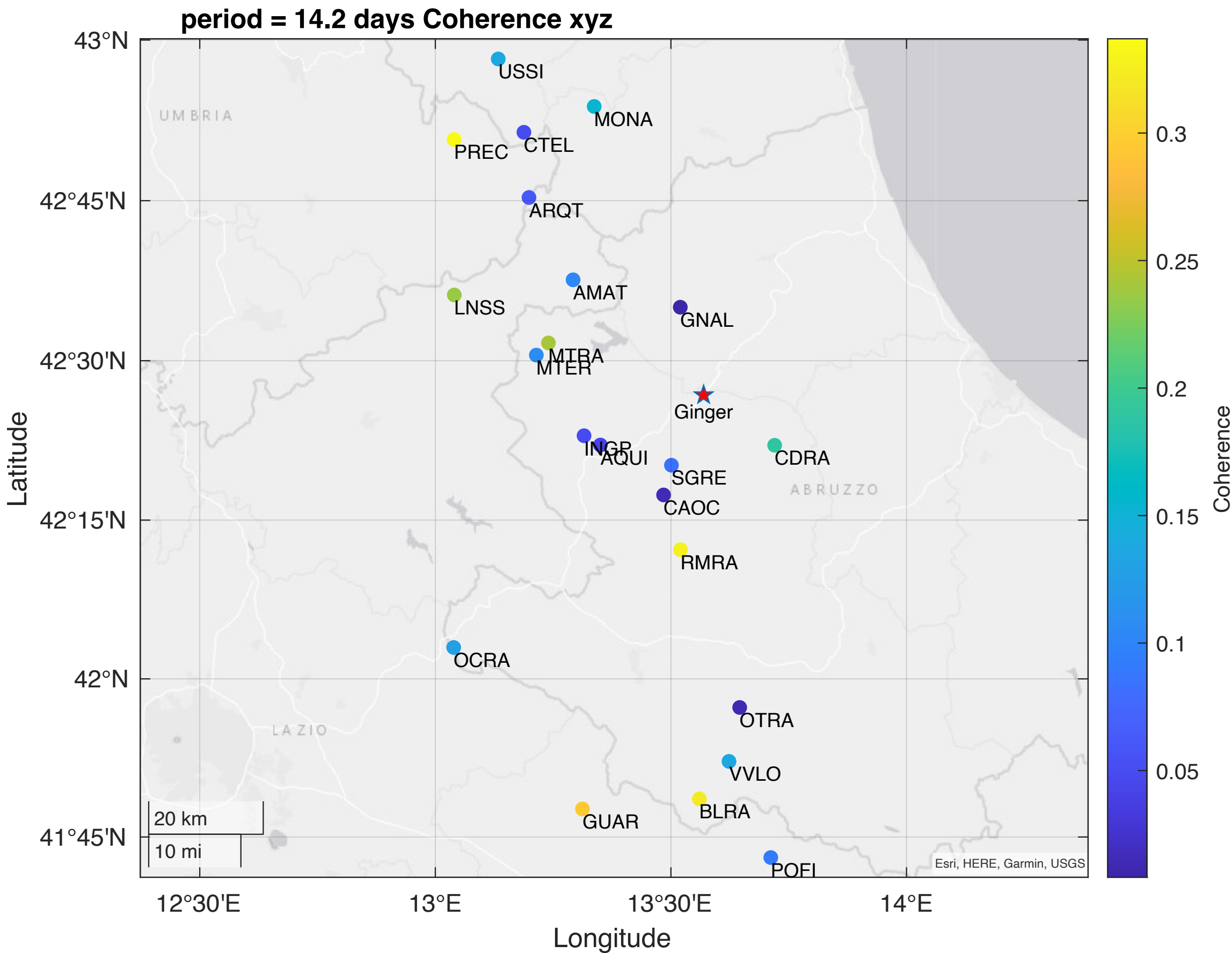
The detection of local deformations is a hot topic in geodesy. In our analysis for the first time a comparison between these instruments has been performed, we compare the signal from Gingerino with the ones from the GNSS stations, homogeneously selected around the position of Gingerino.

Coherence across all time periods



Since we are solely considering the stations and their positions relative to Gingerino, a direct comparison becomes challenging.

Topographical Trend



our focus is on identifying a shared peak among all periods, but no clear topographical pattern emerges.



$$\omega_1 = \frac{|v_1|}{|r_1|} \sin(\alpha_1 - \theta_1)$$

$$v_1 = \sqrt{v_E^2 + v_N^2}$$

$$\alpha_1 = \arctan\left(\frac{v_N}{v_E}\right)$$

$$\sigma_{\omega_1} = \sqrt{\left(\frac{\partial \omega_1}{\partial v_1}\right)^2 \sigma_{v_1}^2 + \left(\frac{\partial \omega_1}{\partial r_1}\right)^2 \sigma_{r_1}^2 + \left(\frac{\partial \omega_1}{\partial \alpha_1}\right)^2 \sigma_{\alpha_1}^2 + \left(\frac{\partial \omega_1}{\partial \theta_1}\right)^2 \sigma_{\theta_1}^2}$$

$\sigma_{r_1}, \sigma_{\theta_1}$ THEY ARE EVALUATED WITH A MONTECARLO METHOD, BECAUSE THEY ARE OBTAINED WITH THE "DISTANCE" FUNCTION OF MATLAB

Using Gingerino position as the pole, the rotational component of each individual station is derived and then the rotation vector associated to the area circumscribed by the stations is obtained by performing a weighted average.



$$\omega_z = \left(\frac{\partial v_x}{\partial y} - \frac{\partial v_y}{\partial x} \right)$$

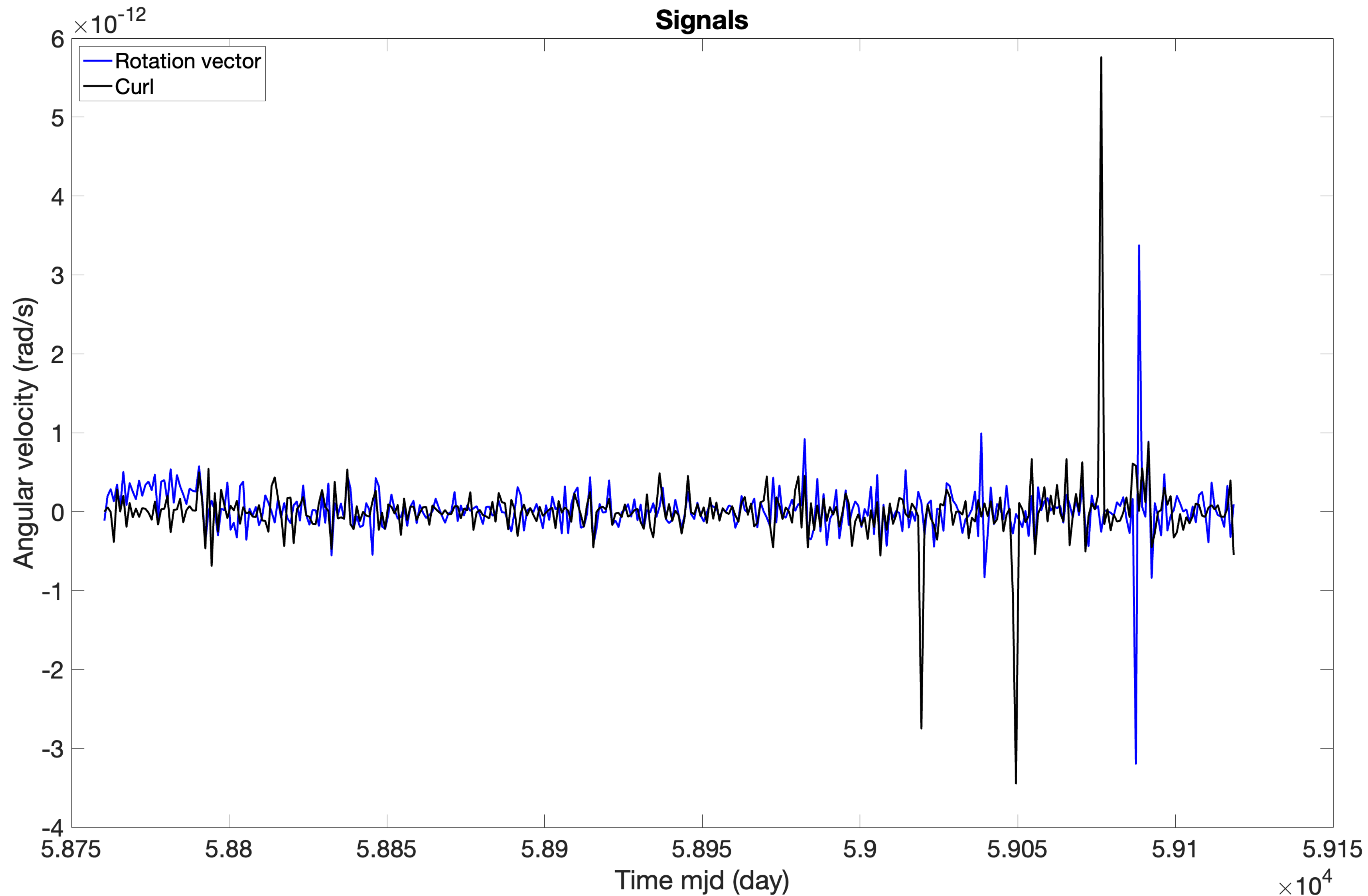
The z-component of the curl of the area circumscribed by the constellation of stations at Gingerino position.

$$v_i = t_i + \frac{\partial v_i}{\partial x_j} x_j = t_i + e_{ij} x_j$$

$$e_{ij} = \epsilon_{ij} + \omega_{ij} = \frac{(e_{ij} + e_{ji})}{2} + \frac{(e_{ij} - e_{ji})}{2}$$

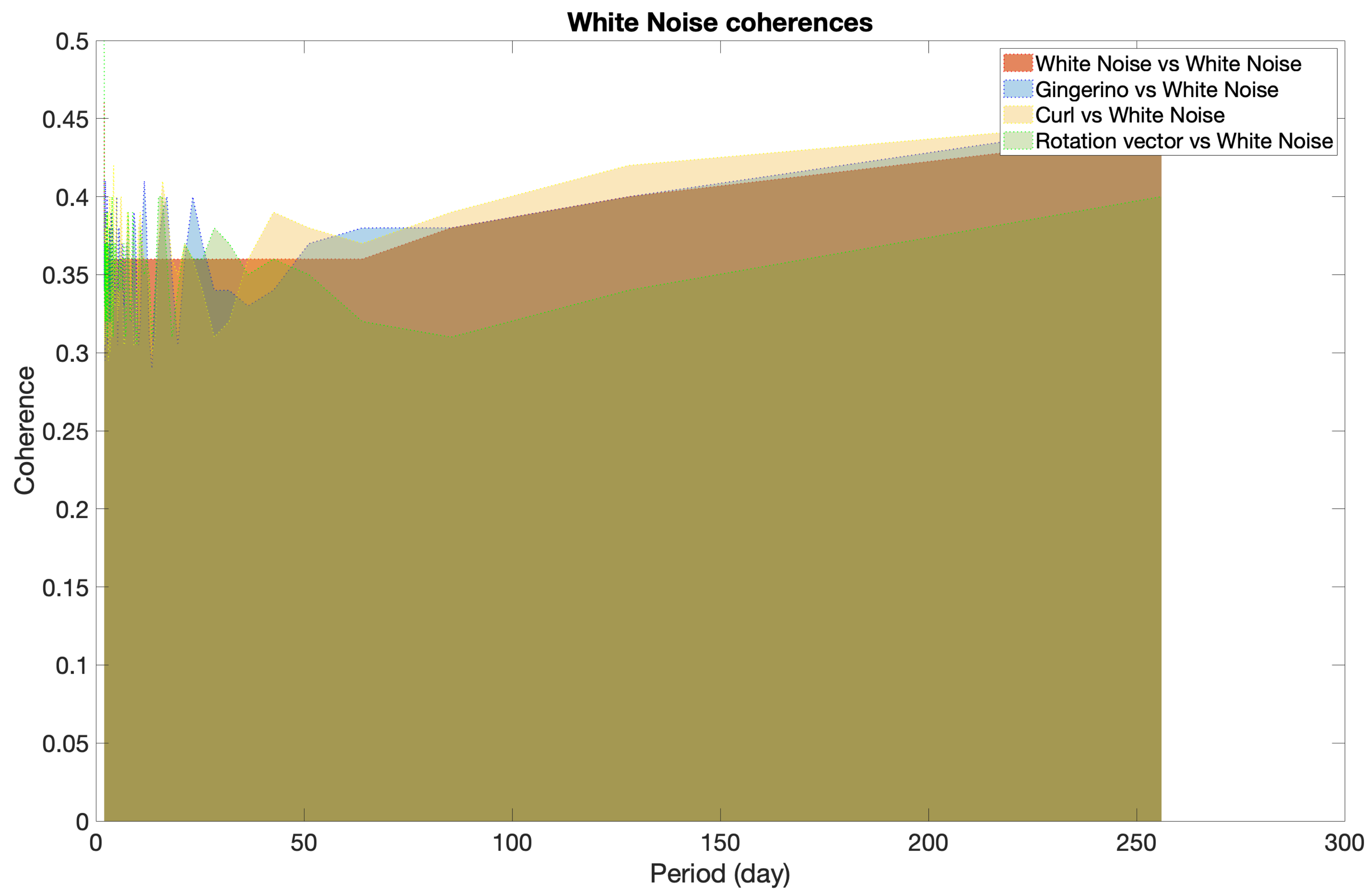
Comparison between the different methods

22



It is noteworthy that the signals obtained, with two different methods, share a common feature: they exhibit identical amplitudes, with some points even reaching peak values, and display coinciding trends.

Baseline for zero coherence: "mscohere"

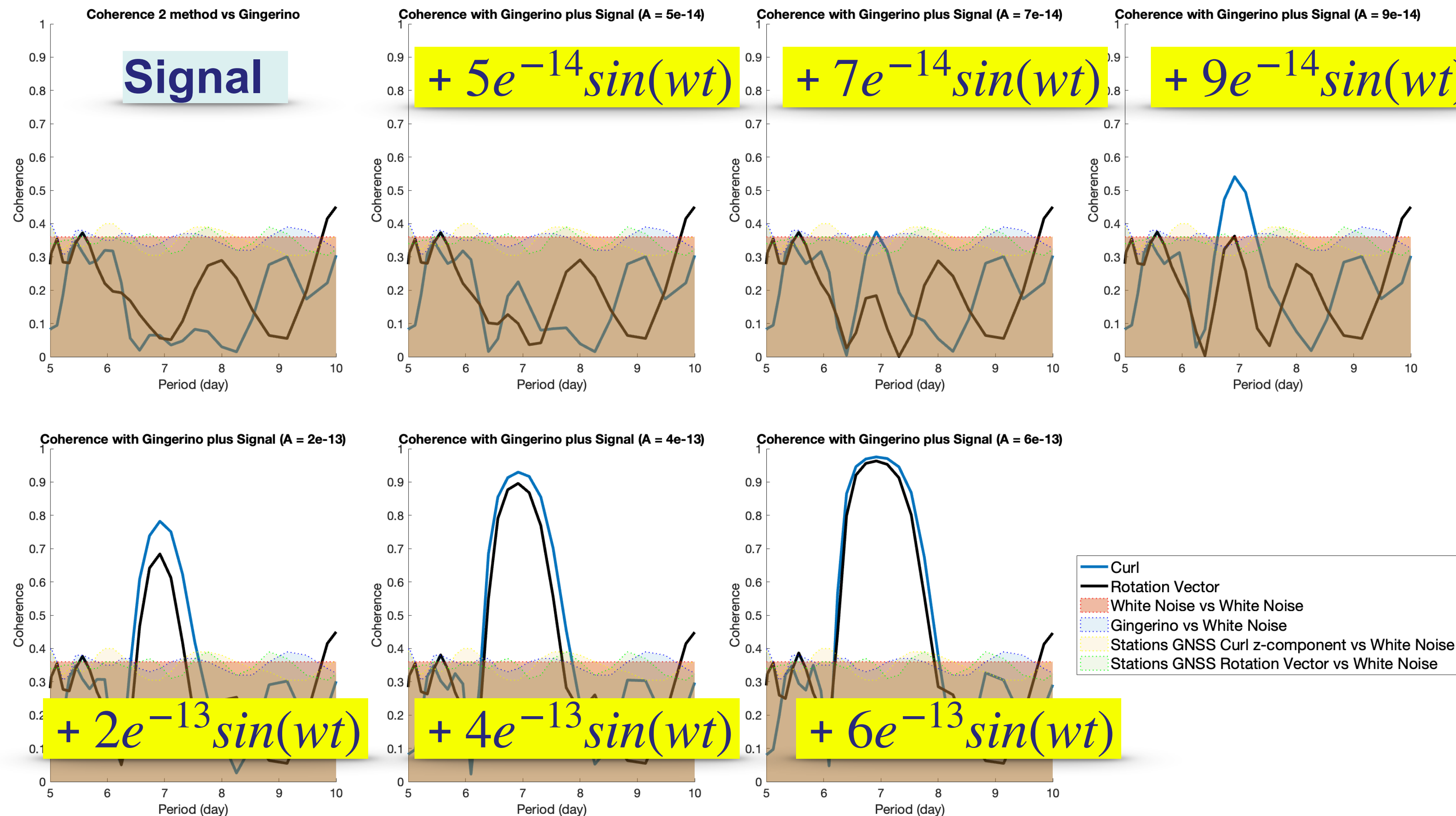


To determine the actual degree of coherence between the two signals, we conducted tests using the **mscohere** function along with simulated white noises. Employing a Monte Carlo simulation approach.

Detection of a synthetic signal at a known frequency 24



We enhanced the angular speeds obtained through the already mentioned methods by introducing a simulated signal that exhibited spikes over a duration of 7 days. This simulated signal had a variable amplitude, reaching up to two orders of magnitude lower than the actual signal.



25





$$\theta = \frac{\pi}{2} - \alpha \quad \gamma = \theta + \frac{\pi}{2}$$

$$f_{TOT} = S\Omega_{\oplus} [\cos(\beta) - (a - b)\sin(\theta)\sin(\beta - \theta) + 2b\cos(\theta)\cos(\beta - \theta)]$$

S is the scale factor of our Sagnac ring

LET'S PUT Z-AXIS LONG \hat{u}_r . SO β , THE ANGLE BETWEEN THE AXIS OF OUR SAGNAC RING AND THE EARTH'S AXIS OF ROTATION, MUST BE PUT EQUAL TO θ :

$$a = 2\frac{m}{r} = 1.3918082245(20) \times 10^{-9}$$

$$f_{zTot} = S\Omega_{\oplus} [\cos(\theta) + 2b\cos(\theta)]$$

Earth's rotation

Lense-Thirring effect

$$b = \frac{GI}{c^2 r^3} = 2.301326(700) \times 10^{-10}$$

PUTTING Z-AXIS LONG \hat{u}_θ WE HAVE THAT $\beta = \gamma = \theta + \frac{\pi}{2}$
(ATTENTION IS DOWNWARDS):

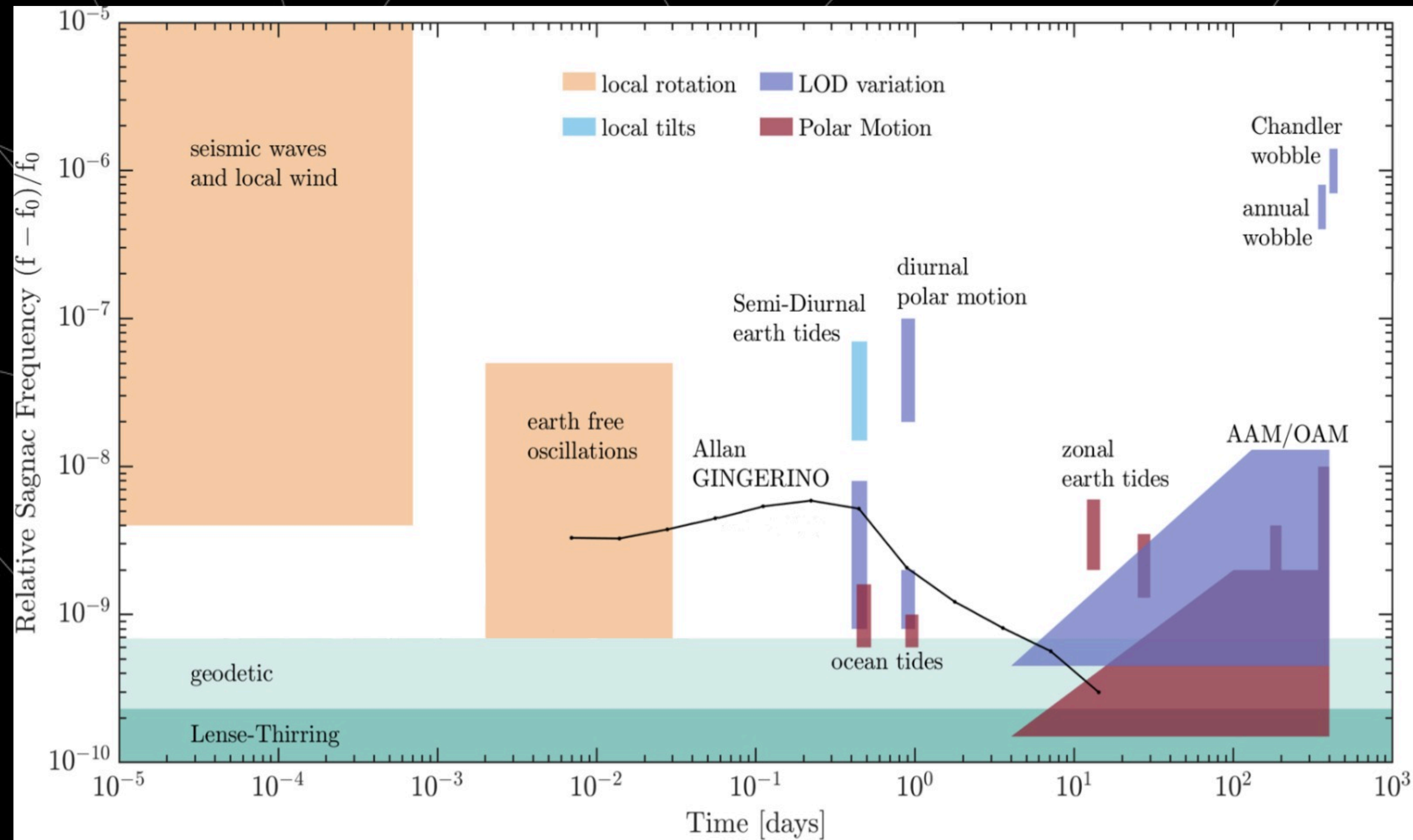
$$f_{xTot} = S\Omega_{\oplus} [-\sin(\theta) - a\sin(\theta) + b\sin(\theta)]$$

Earth's rotation

deSitter effect

Lense-Thirring effect

Allan deviation

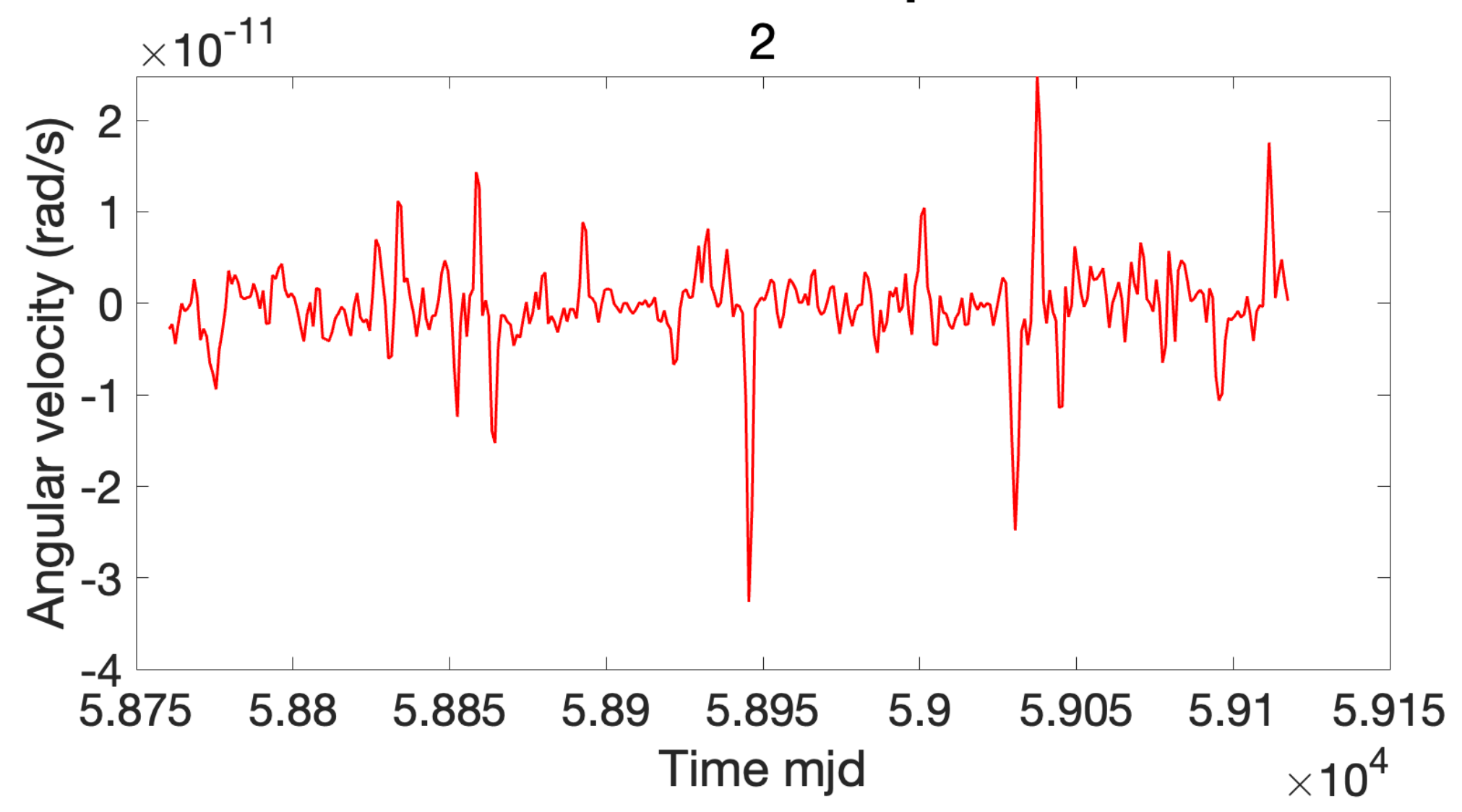


GINGER sensitivity targets: 1 part out of $10^9 - 10^{11}$ of the Earth's rotation
1 part out of 10^9 is the fundamental physics watershed



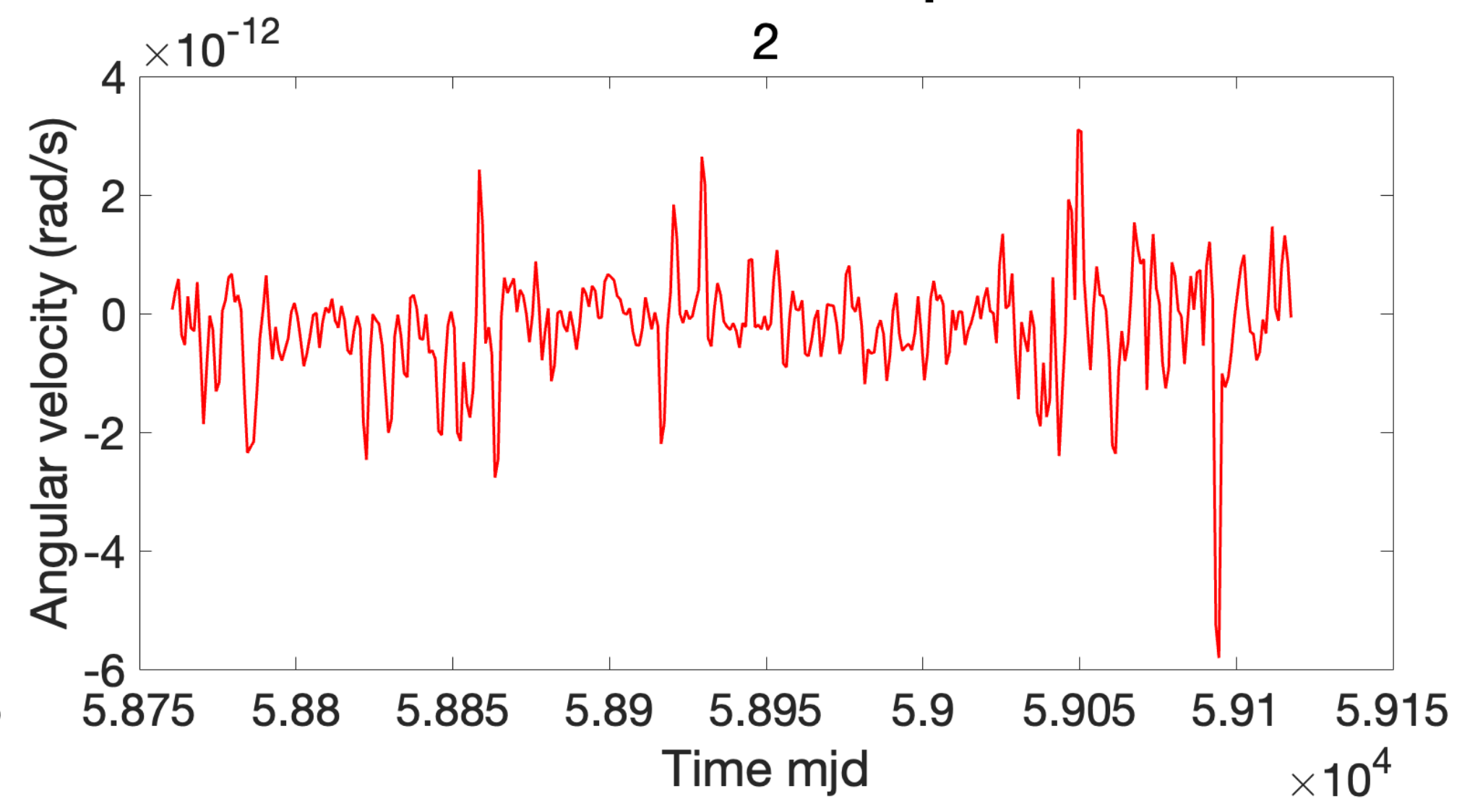
GINGERINO L pt

2



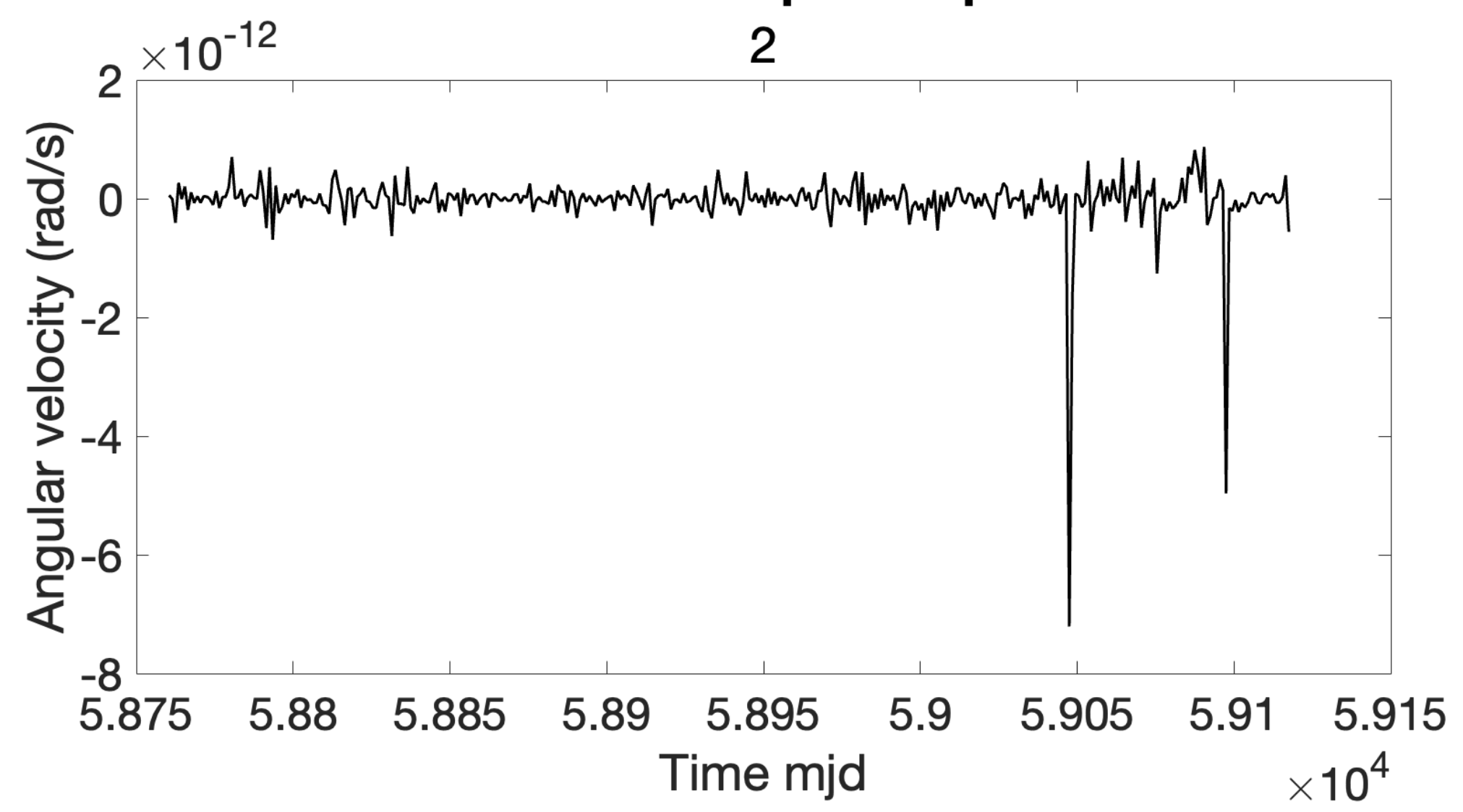
GINGERINO TL pt

2



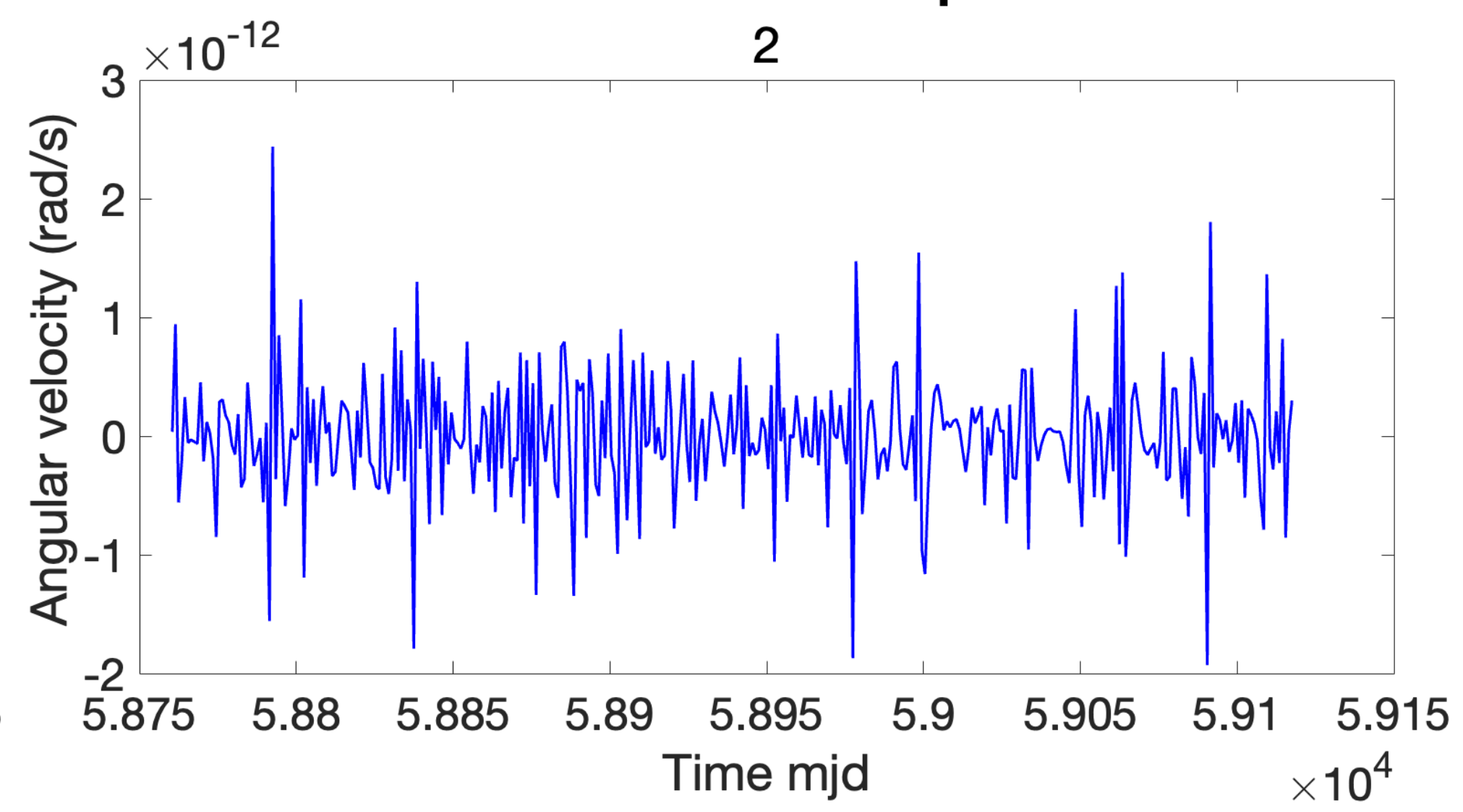
Curl z-component pt

2



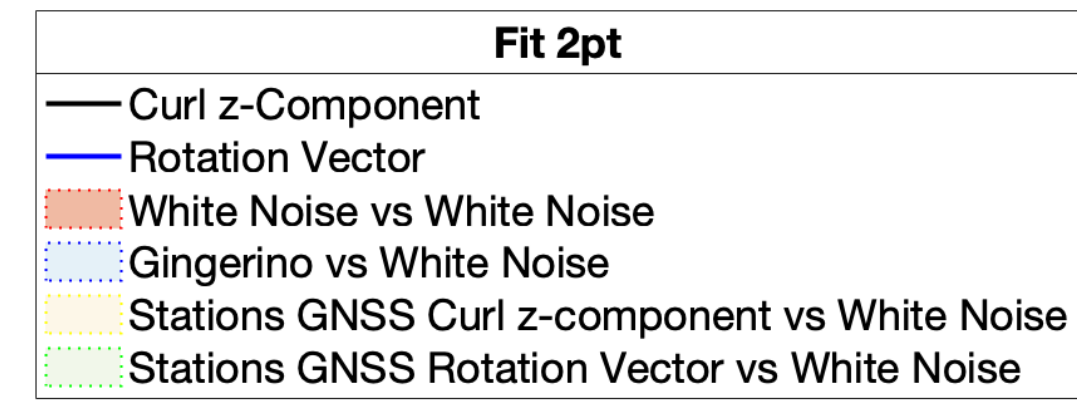
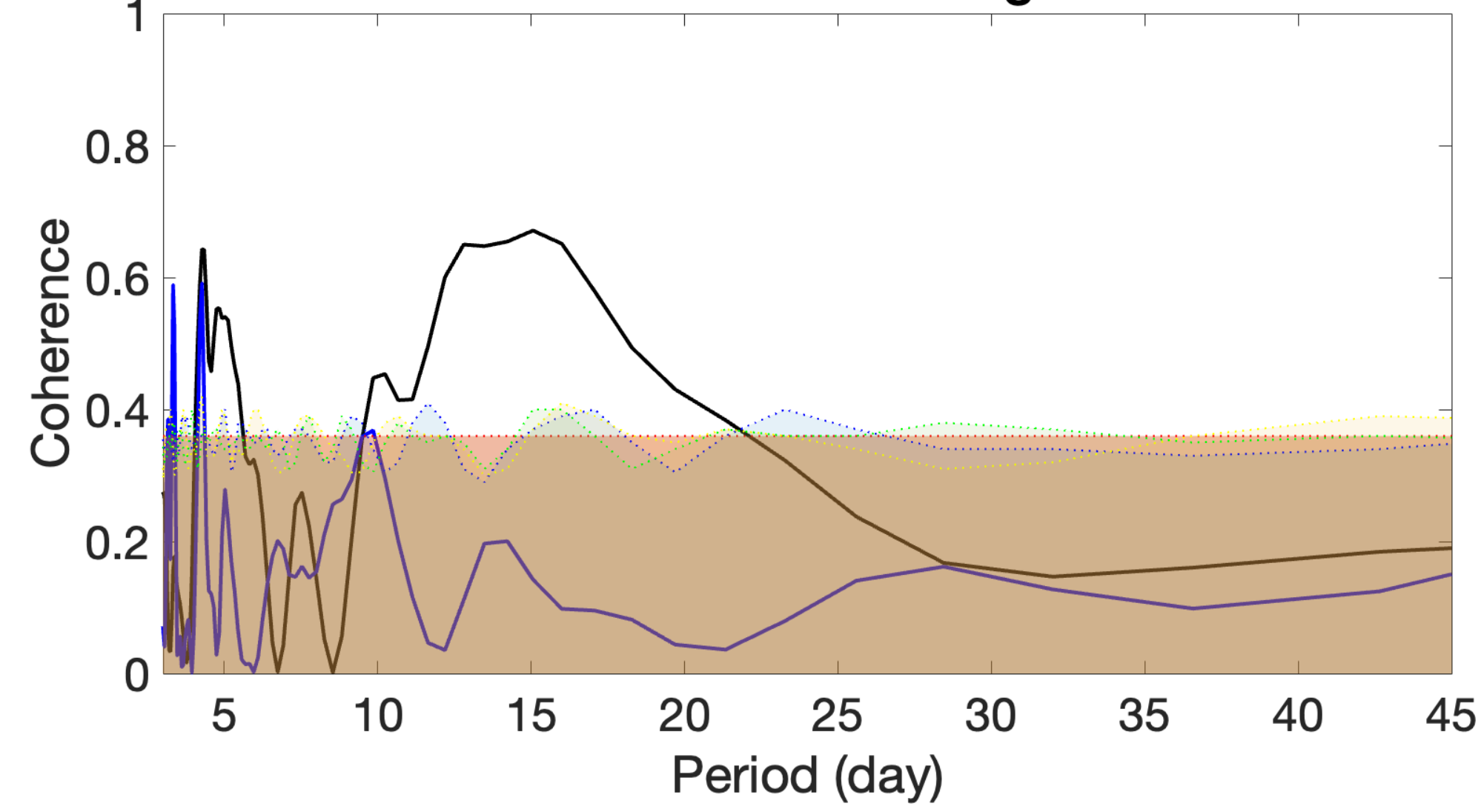
Rotation Vector pt

2

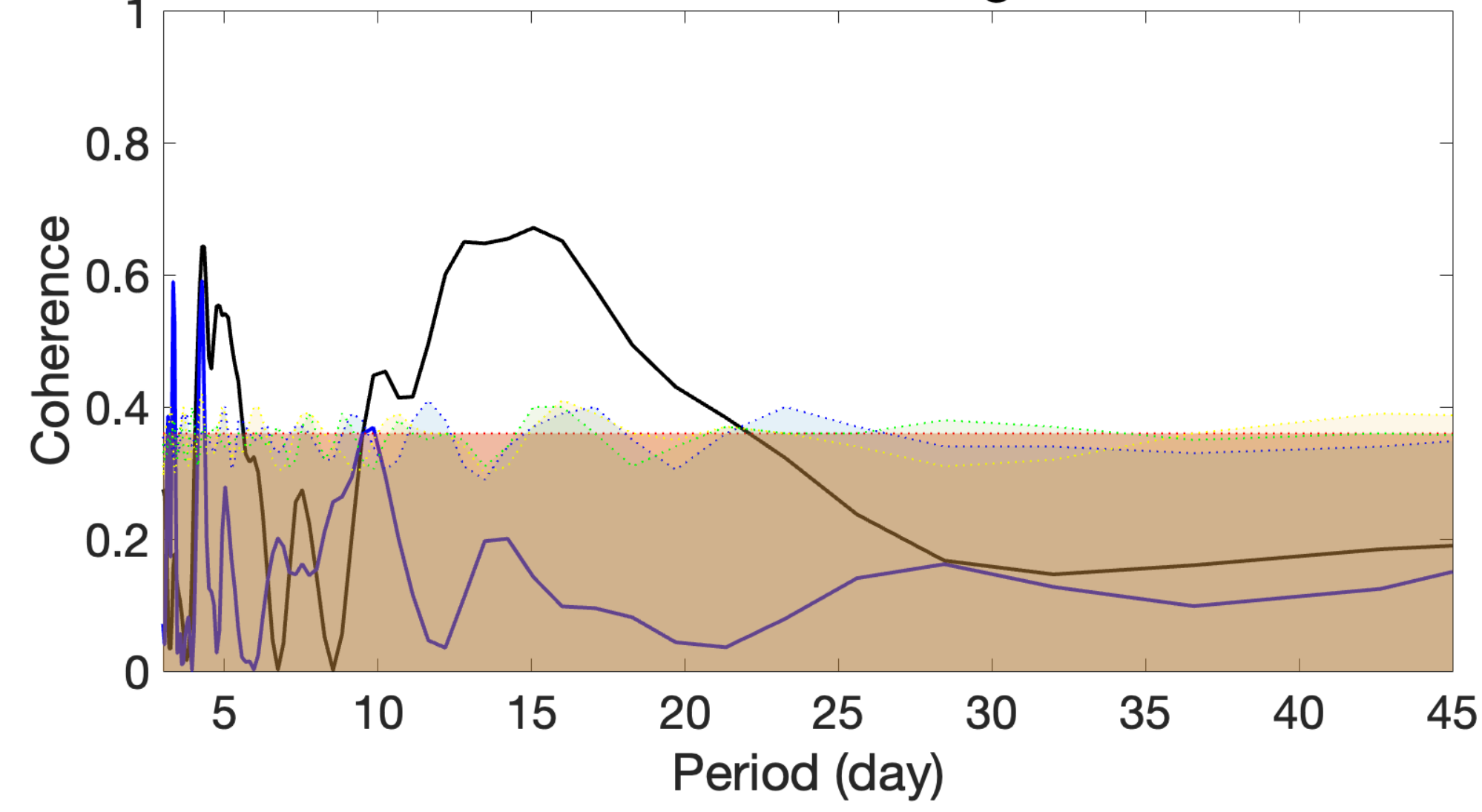




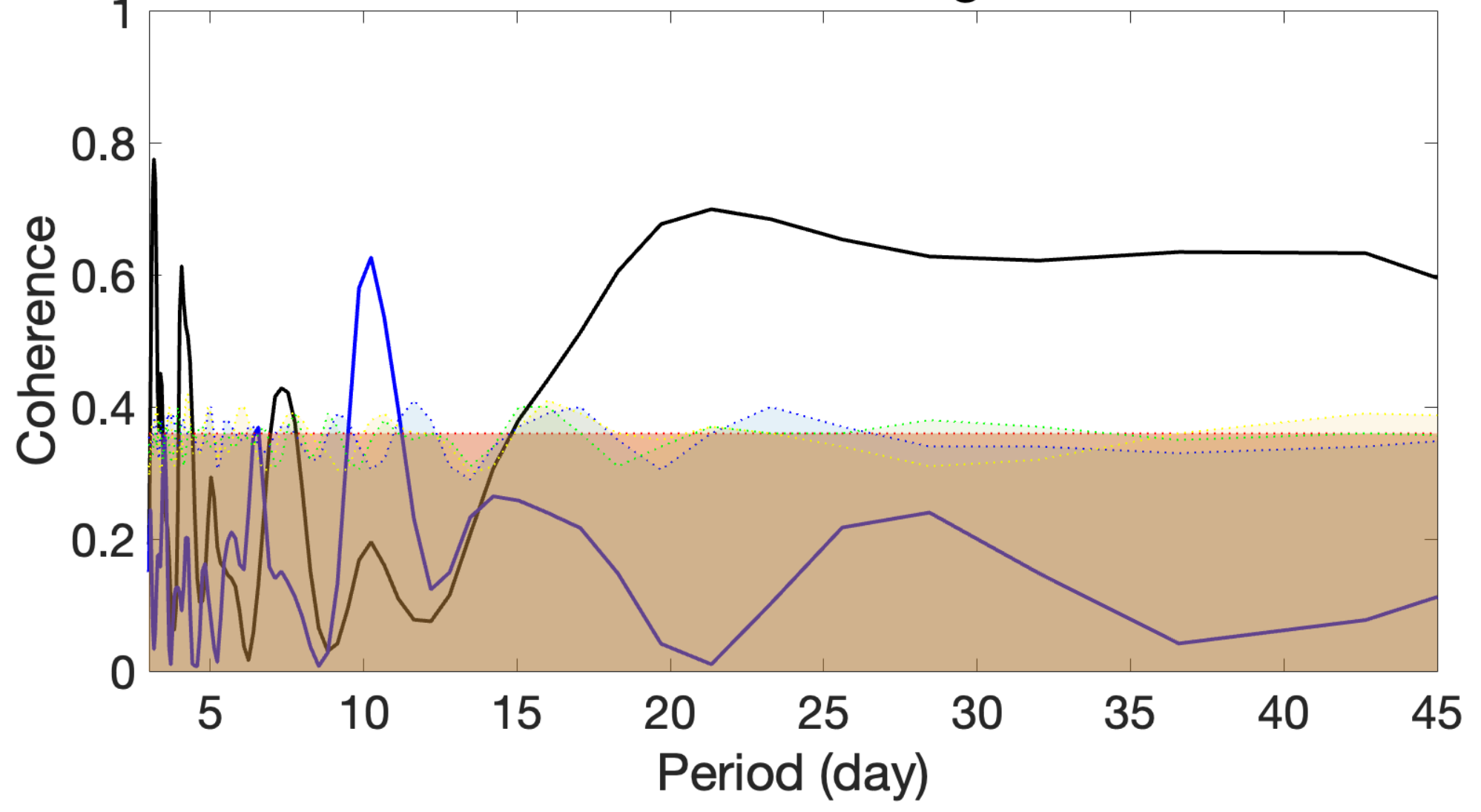
All the methods vs Gingerino



All the methods vs Gingerino L



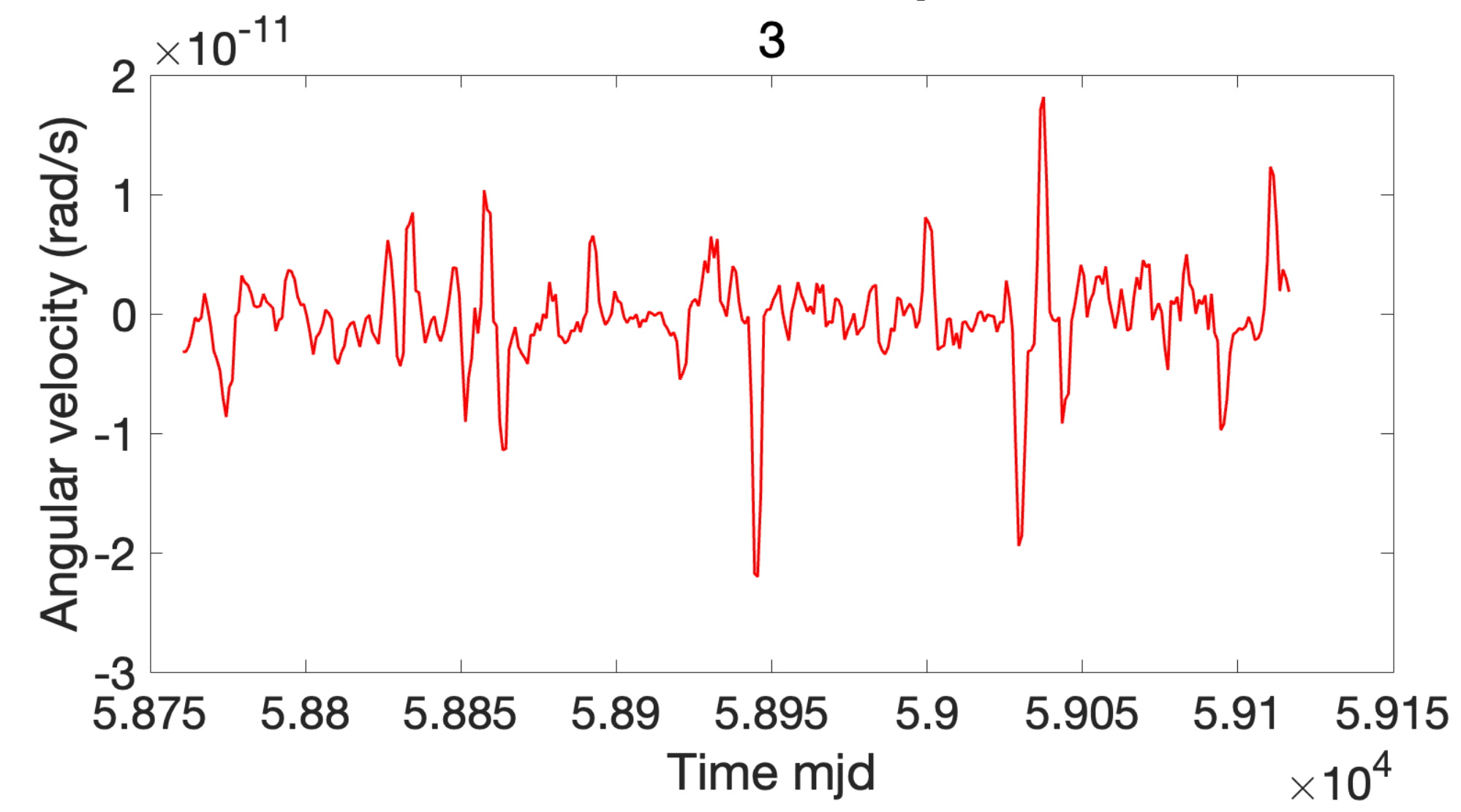
All the methods vs Gingerino TL





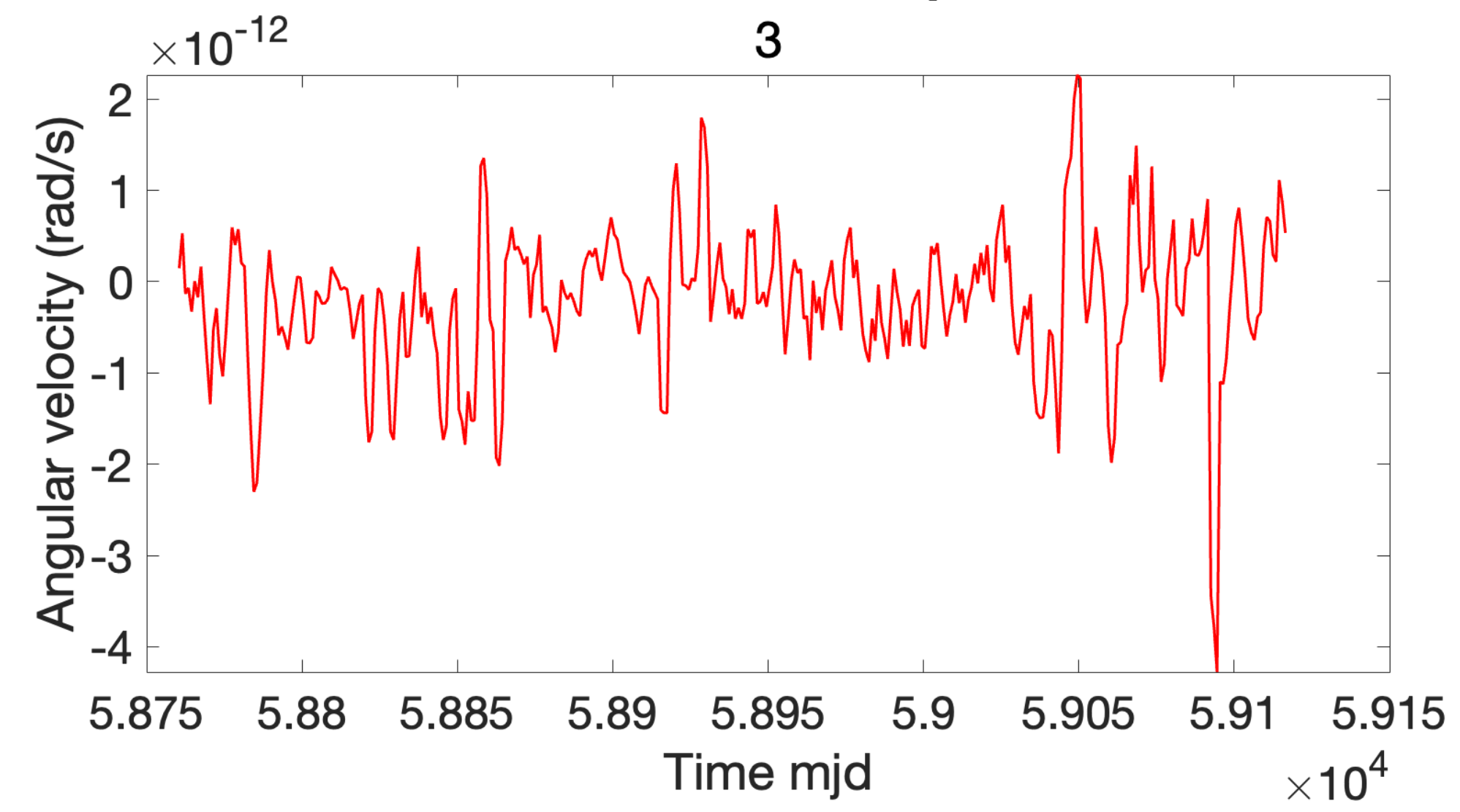
GINGERINO L pt

3



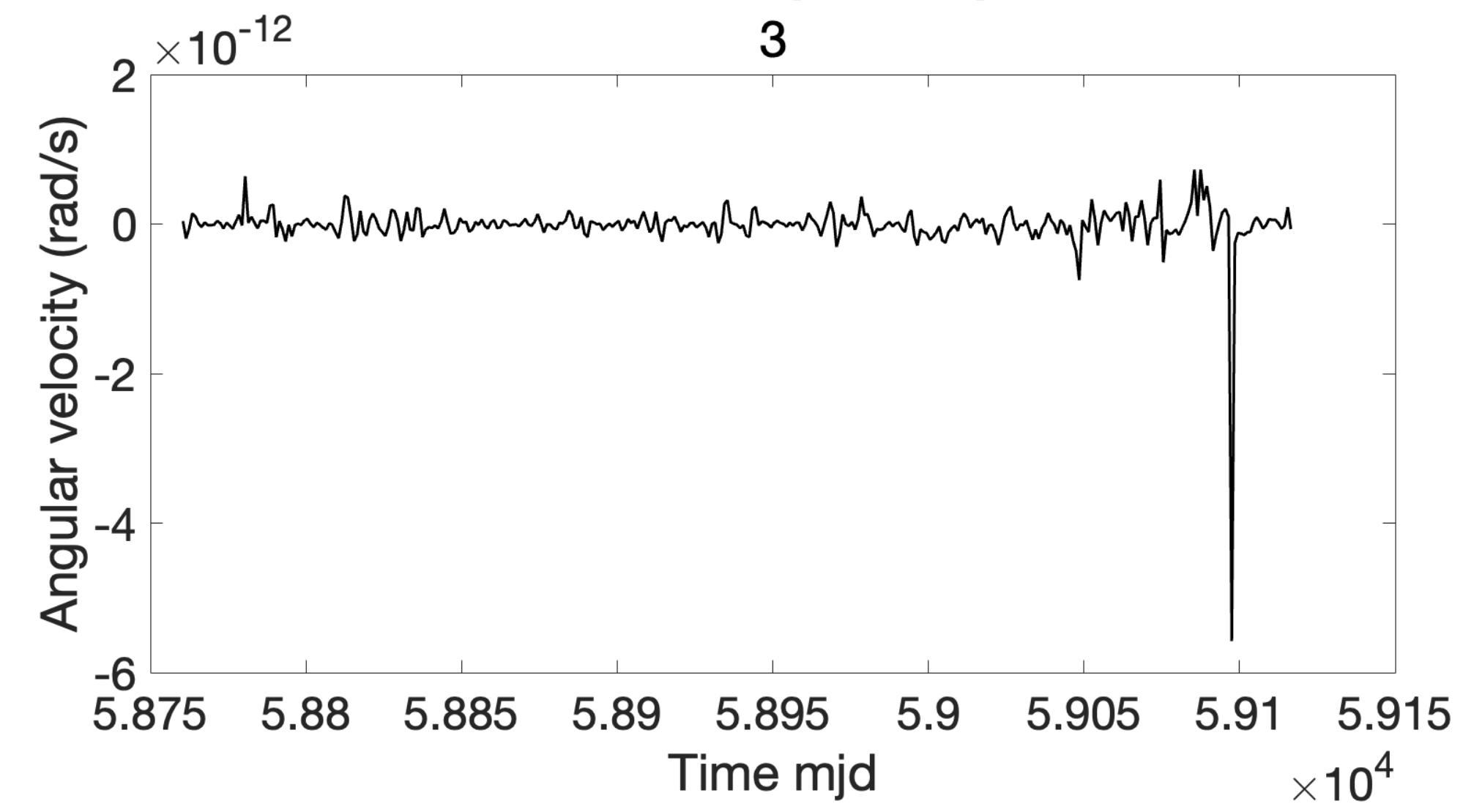
GINGERINO TL pt

3



Curl z-component pt

3



Rotation Vector pt

3

